An extensible simulation environment and movement metrics for testing walking behavior in agent-based models

Torrens, Paul M. [€,1] Email: torrens@geosimulation.com

Nara, Atsushi. [1] Email: atsushi.nara@asu.edu

Li, Xun. [1] Email: Xun.Li@asu.edu

Zhu, Haojie. [1] Email: Haojie.Zhu@asu.edu

Griffin, William A. [2] Email: WILLIAM.GRIFFIN@asu.edu

Scott B. Brown. [3] Email: scott.brown@spatial-reasoning.org

[€]To whom correspondence may be addressed.

[1]Geosimulation Research Laboratory and GeoDa Center for Geospatial Analysis and Computation, Box 875302, School of Geographical Sciences & Urban Planning, Arizona State University, Tempe, AZ 85287-5302, USA

[2]Center for Social Dynamics and Complexity, Box 876505, Arizona State University, Tempe, AZ 85287-6505, USA

[3] Idaho National Laboratory, 2525 Fremont Ave., Idaho Falls, ID 83402-1509, USA

Research highlights

- We present a novel approach to testing, evaluating, and playing with rules for walking behavior in agent-based simulation, using an extensible framework for model development that allows for a variety of heuristics, algorithms, and approached to be experimented with in simulation, and a set of metrics that allow relative movement to be measured and compared between models and with the real-world.
- Our approach extends the capabilities of movement exploration in agent-based simulation by introducing a more extensible modeling scheme that can be applied across application scenarios, cities, and scales.
- We prove the usefulness of the scheme by evaluating a suite of commonly-deployed movement models/routines used in simulating movement at different scales.

Revised manuscript
Click here to view linked References

An extensible simulation environment and movement metrics for testing walking behavior in agent-based models

"*Watching all the insects march along / Seem to know just right where they belong.*" (Reznor, 2005)

Abstract

Human movement is a significant ingredient of many social, environmental, and technical systems, yet the importance of movement is often discounted in considering systems' complexity. Movement is commonly abstracted in agent-based modeling (which is perhaps *the* methodological vehicle for modeling complex systems), despite the influence of movement upon information exchange and adaptation in a system. In particular, agent-based models of urban pedestrians often treat movement in proxy form at the expense of faithfully treating movement *behavior* with realistic agency. There exists little consensus about which method is appropriate for representing movement in agent-based schemes. In this paper, we examine popularly-used methods to drive movement in agent-based models, first by introducing a methodology that can flexibly handle many representations of movement at many different scales and second, introducing a suite of tools to benchmark agent movement between models and against real-world trajectory data. We find that most popular movement schemes do a relatively poor job of representing movement, but that some schemes may well be "good enough" for some

applications. We also discuss potential avenues for improving the representation of movement in agent-based frameworks.

Keywords: walking, agent-based modeling, movement, trajectory measurement

1 Introduction

Movement of pedestrians is significant across a variety of domains in which it is infeasible to experiment with real people or environments. As an alternative, *agent-based models* (Russell and Norvig, 1995), which date to Alan Turing's original work on intelligent machines (Turing, 1950), are popularly used to generate synthetic pedestrians in simulation. In many instances, however, representation of agent movement in models is cursory compared to our understanding of the factors that drive human motion in the real world and little robust investigation of the plausibility of pedestrian movement in agent-based models has been performed. Rather than deriving from *behavior*, pedestrian agent-based models are often developed from the *physics* or *informatics* of movement. The reasoning for this is straightforward: motion is well-understood in these domains. However, there exists little basis for developing consensus among the builders of agent-based models regarding the implications of choosing one movement algorithm over another. It is also troublesome, philosophically, when models of human movement bear little behavioral resemblance to reality, but are used to inform decisions.

The question that we pose in this paper is: *which algorithms are appropriate proxies for human movement in agent-based models and why*? With this in mind, we critically examine movement

algorithms commonly employed in agent-based pedestrian models, assessing their fit with theory, with each other, and—using traces of real human movement—with reality. Answering this question first requires that we develop an extensible agent-based modeling platform that can realize multiple models, algorithms, and parameters. Second, it requires that we introduce methods to assess the relative performance of movement algorithms and their ability to replicate real-world paths. We will demonstrate that, with few exceptions, movement algorithms for agent-based models do a relatively poor job of reproducing realistic mobility in simulation. Some algorithms are perhaps "good enough" as rough proxies for human movement, but this generally holds only for particular types of sub-movement, at particular scales, or in specific environments. We examine why this might be the case and what might be done to remedy the problem.

2 Related work

A variety of approaches have been developed to handle pedestrian movement in agent-based simulations. *Physics models* often work from the assumption that agents "go with the flow" of an ambient crowd and that their motion can be modeled using equations for flow of non-human media such as gases or fluids (which are more tractable that the "messy complexity" of people). A related assumption is often made: that pedestrians might cede their personal movement behavior to that of the crowd in very densely-populated streetscapes (Hoogendoorn and Bovy, 2000; Moussaïd et al., 2009), because of reduced degrees of freedom or in extreme scenarios where panic induces stampedes (Vicsek, 2003). A variety of techniques are used to model flow and person-scale movement within the "stream" is usually represented as particle interactions with frictional or force effects. The equations may represent Brownian motion, (Schweitzer, 2003), random-walks (Batty, 2003; Keßel et al., 2002; Nagatani and Nagai, 2004; Tecchia et al.,

2002), or Lévy-flights (Jiang and Jia, 2009). Other approaches use continuum mechanics in a field-space or vector-space (Chenney, 2004), using Maxwell-Boltzmann equations (which describe gases: see Henderson, 1971 for a pedestrian movement example) or Navier-Stokes equations (which describe fluids: see Hughes, 2003; Treuille et al., 2006) that represent the motion of the continuum from its constituent parts. Because agents in these schemes are characterized homogenously, the equations can be used to generate many-to-many interactions in large simulated crowds, with relative economy in computation (see the performance savings reported in Patil et al., 2010, for example).

Path-based heuristics follow graph-traversal schemes developed in computer science. Often, pedestrian environments are represented as a tessellated space (Gipps and Marksjö, 1985), which agents traverse by scanning probable "next-steps" and assessing the contribution of step-options to the overall path length (Nieuwenhuisen et al., 2007), visibility (Turner and Penn, 2002), biomechanical effort (Guy et al., 2010), or other conditions.

Cellular automata models usually ascribe pedestrians to cells using state-descriptors, such as density of occupation (Gipps and Marksjö, 1985), and those states are diffused by exchange with neighboring cells using transition rules, usually as myopic graph-searches that mediate the value of a given cell in a previous time-step with state (pedestrian density, walkability) information in the ambient neighborhood (Blue and Adler, 2001; Crooks et al., 2009). In some instances, cells are designed to represent individual pedestrians and state information such as velocity and speed may be shared between cells (see Kukla et al., 2001, for example).

Data-mining and knowledge discovery may be used to source agents' movement from libraries of trajectory samples (Lee et al., 2007; Lerner et al., 2007). These samples may come from

location-aware hardware that pedestrians may carry, or from image processing of video sequences to extract movement trails (Kitazawa and Fujiyama, 2010).

Agency-driven models usually seek to mimic socio-behavioral agency (decision-making, motivation, affect; see Pelechano et al. (2008) for an overview) in movement or to treat cognitive functionality such as memory (Sakuma et al., 2005) or vision (Boulic et al., 1994; Renault et al., 1990). In other examples, collective agency is considered, as interactions among pedestrians in crowds, either as "herds" (Reynolds, 1987), as social groups (Musse and Thalmann, 1997) or as teams (Allbeck et al., 2002).

Perhaps due to the difficulties of collecting data in large crowds and in natural contexts, *formal analysis of movement in agent-based models* is performed relatively infrequently. There are some exceptions: Singh, et al (2009) developed performance tests for agent steering in simulation, as well as a set of metrics for measuring steering, although these were not compared to real-world data. Dodge *et al.* (2009) cataloged a set of physical characteristics that can be used to index movement in moving objects databases. Jiang *et al.* (2009) introduced a scheme for relating pedestrian mobility to urban street networks. The descriptive properties of crowd flow are by far the most common metric for agent-pedestrian models, because they ally with policy-relevant characteristics such as occupancy levels (Fruin, 1971), crowd density (Batty et al., 2003a), flow rates (Henderson, 1971), and egress timing (Nara and Torrens, 2007). The presence of emergent patterns in crowd flow—lane-formation (Helbing and Molnár, 1997), vortices (Venuti et al., 2007), annealing (Zhang, 2009), and bottlenecks (Hoogendoorn and Daamen, 2005)—are also explored because they have been observed in video footage of real crowds (Johansson et al., 2008; Moussaïd et al., 2009).

While a wide variety of approaches are available as movement regimes for agent-pedestrians in simulation, relatively little effort has been invested in benchmarking the suitability of individual movement algorithms to real-world data, or in relating algorithms to each other. This is perhaps a consequence of the disparate models used, which often focus on specific sub-movements (trip-determination, path-planning, navigation, way-finding, steering, collision avoidance, locomotion). This begets the following questions: which movement algorithms are suitable analogs for real-world behavior and how might we determine this qualitatively and quantitatively? To answer this, we have developed an agent-based platform that can flexibly accommodate varying representations of movement. Any differences in movement can be attributed to the algorithm, thus avoiding potential modeling artifacts or differences in running models over different platforms or data models. We have also developed a scheme to measure movement across application domains, across movement characteristics, and across scales. We have chosen to test the following movement algorithms, because they represent a full spectrum of movement behaviors and relevant scales; they are also commonly used in agent-based models: simple random walk, Brownian motion, Lévy-flights, hopping, path-planning, greedy hill-climbing, steering, and social force.

3 Methods

In this section, we will introduce an extensible automata scheme for modeling movement. We will also detail how we fit common algorithms to this framework.

3.1 A flexible information architecture for agent movement

Our agent-based platform uses geographic automata (Torrens and Benenson, 2005) as the information handler for motion control. Geographic automata (GA) provide the extensibility necessary to develop a diverse set of movement algorithms across varying conceptualizations of space, situational awareness, and information-processing in simulation. Geographic automata contain all of the "standard" information-processing of agent-automaton (states S, state transition rules R_S, and neighborhoods of input/interaction N), but they add specialized functions for handling geography.

$$
\begin{aligned}
&GA = \{K, S, R_S, L, R_L, N, R_N\} \\
&\text{State transition rule: } R_S: S(t) \rightarrow S(t+1) \\
&\text{Movement rule: } R_L: L(t) \rightarrow L(t+1) \\
&\text{Neighborhood rule: } R_N: N(t) \rightarrow N(t+1)
\end{aligned}
\tag{i}
$$

A movement ontology K allows a user to characterize (or other automata to interpret) automata as mobile or stationary; if stationary, movement rules are not applied. Locations L are used to encode positions using a *variety of spatial conventions*. *Cell-space* is used to divide a space into discrete rasters. *Vector-spaces* register agents' position within a field-space. *Graph-space* is used to position agents within a network $G = (V, E)$ of vertices V and edges E. *Metric-space* is used to cross-index the other three spaces to Euclidean geometry. An agent may therefore be positioned in multiple spaces at once. Movement rules R_L articulate agents through L and time t.

Neighborhoods N encapsulate portions of space and time in L, usually for the purpose of gathering state information within space-time envelopes. For cell-spaces, neighborhoods are defined as discrete areas of a lattice, centered on an agent. For vector-space neighborhoods, any Euclidean object can be designated as a neighborhood and agents may assess it with Euclidean or topological operators. Neighborhoods in graph-space are expressed as an adjacency-list of in-edge and out-edge connections with other vertices (or graphs). The relationships N are "dockable": agents may poll neighborhood information from many of the space protocols in the model. Neighborhood rules R_N allow specification of mechanisms for changing neighborhood conventions over space and time (in conjunction with state transition rules R_S and/or movement rules R_L).

3.1.1 Memory

Agents retain a short-term memory structure, implemented as arrays and organized hierarchically using queues. Priority queues can thus be specified and information can be loaded to these queues or removed from memory using standard "pop" and "push" schemes (Lormen et al., 2007). Agents may also share their queue information with other agents.

3.1.2 Timing

Two types of update cycle are allowed in the model. The first option is asynchronous, which introduces a stochastic element into the order in which agent states, locations, and neighborhoods are updated in the duration $t \rightarrow t + 1$. The second option uses a "sloppy synchronous" (Watkinson, 2002) update: agents are updated in the order in which they were created.

3.2 Software overview

The software scheme for the model is illustrated in Figure 1. An "agent factory" allows users to introduce customized agents in simulation. Parameters for simulation may also be customized and read-in at run-time or on-the-fly. Spatial objects and relationships are managed via a geographic information system (GIS), which facilitates data access and can be used to introduce neighborhood filters. Probe agents are used to poll information from the model during run-time and these data may be visualized or run through validation metrics. Simulations are visualized in run-time (Figure 2) using the OpenGL components of Reynolds's Opensteer library (1999) (it is important to state that our model is decoupled from Reynolds's steering model; we only use the *graphics libraries* for display); in addition, we added a scene graph to manage the rendering of objects dynamically on-screen.

[Figures 1, 2 go here.]

3.3 Movement by path-planning

We considered three algorithms for path-planning: a hill-climbing algorithm (Figure 3), Dijkstra's algorithm (Figure 4), and A* search (Figure 5). Hill-climbing is a greedy goal-seeking behavior: it produces a path from source to sink in a graph by iteratively exploring nodes. This is usually *myopic*. At a given node, the algorithm assesses adjacent nodes (locally, e.g., within a five-cell von Neumann or nine-cell Moore neighborhood) and moves the agent to the node that it determines to be nearest the global sink *at that point in time*.

[Figures 3 to 5 go here.]

Dijkstra's (1959) algorithm finds *a* (not necessarily *the*) shortest path from an origin to a destination, using incremental expansion to adjacent vertices on a graph (best-first search). It differs from hill-climbing by considering its *entire search history* at any given time. At each expansion point, the algorithm calculates and stores its progression from the origin. The algorithm also remembers where it has been and what nodes it still needs to visit. Once it has visited all vertices on the graph, it selects a path that has the shortest total edge length from the origin to the destination. Movement along this path can then proceed along edges (u, v) separating individual nodes u and v. The algorithm is detailed in Table 1.

[Table 1 goes here.]

The A* algorithm (Hart et al., 1968) is similar to Dijkstra, but in addition to calculating $d[n]$ at each choice-point n in the search, A* also calculates the Euclidean distance from a given node to the destination (in addition to graph distance) when estimating the plausibility of a given node's candidacy for the shortest path S_{list}. For this to work, the graph G must be metric. Euclidean distance is used because it represents the shortest possible path between two nodes. The heuristic allows A* to prune unlikely paths from the search, by comparing progress *from* the origin s (as in Dijkstra's algorithm) with estimated progress *to* the destination (the true value of which is unknown with certainty until the destination is reached). Plausibility is calculated as follows.

$$f^*(n) = g^*(n) + h^*(n) \quad \text{(ii)}$$

Above, $f^*(n)$ is the estimated plausibility of a given node $n \in V$, $g^*(n)$ is the estimated progress from the origin s, and $h^*(n)$ is the estimated Euclidean distance from node n to the destination (where $h^*(n) = 0$ at the destination node). Given a choice between nodes $n_1, n_2, \ldots, n_k$ to add to a shortest path list S_{list}, the A* algorithm will select the node with the smallest associated $f^*(n)$.

3.4 Movement by random walk

Random walks move agents by perturbing their trajectory in motion, sometimes following some probability distribution that expresses the propensity for the agent to move with a particular heading. We considered three distinct types of random walks: a simple random walk (Figure 6), Brownian motion (Figure 7), and a Lévy-distributed walk (Figure 8). The walks are performed as vector movements over a field-space. In each case, agents begin their walks from a randomly-assigned start position within the field.

The *simple random walk* determines an agent's new location (x, y) between time steps $t \to t + 1$ as follows:

$$x(t+1) = x(t) + (\delta \cos\theta)$$
$$y(t+1) = y(t) + (\delta \sin\theta) \qquad \text{(iii)}$$

Movement is linear and the step-size δ is user-defined (we used a value of $\delta = 1$); direction for movement $(0 \leq \theta < 360)$ is selected randomly.

[Figure 6 goes here.]

Brownian motion generates stochastic random walks by assuming that movement is influenced by an ambient liquid in continuous time. We modeled Brownian motion using a set of differential equations, following the Langevin approach described in Schweitzer (1997) :

$$\frac{dr}{dt} = v$$
$$\frac{dv}{dt} = -\gamma v + \sqrt{2\varepsilon\gamma}\xi(t) \quad \text{(iv)}$$

Equation (iv) updates the position $r(t)$ of an agent at time t by manipulating its velocity $v(t)$; the liquid is represented by a random function $\xi(t)$; γ is a friction coefficient and ε is the intensity of a stochastic force (Gaussian white noise). These parameters are user-defined: we used $\gamma = 0.9$, $\varepsilon = 0.5$, and $t = 0.01$.

[Figure 7 goes here.]

Lévy flights generate movement of varying lengths (Figure 8), while maintaining a scale relationship between lengths, using a Lévy index, an exponent $(1 < \mu \leq 3)$, which follows a power-law distribution. The exponent is introduced to agent movement as follows (Bartumeus et al., 2005):

$$length = \Delta t \left(10 \cdot \text{uniform}(0,1)^{\frac{1}{1-\mu}}\right) \quad \text{(v)}$$

μ is the Lévy index, which may be user-defined (we used $\mu = 1.6$ and $t = 0.01$).

[Figure 8 goes here.]

3.5 Movement by steering

Movement by steering is usually based on Newton's (1687) first and second laws of motion, which treat acceleration by applying force relative to mass. We calculated linear and angular acceleration forces by updating agents' velocity/rotation (v) and position/orientation (p) through Euler integration of acceleration (a) over $t \rightarrow t + 1$, as follows:

3.6 3.7 $$\vec{v} = \vec{v}_0 + \vec{a} \cdot \Delta t$$ (vi)

3.8 $$\vec{p} = \vec{p}_0 + \vec{v} \cdot \Delta t$$

3.9 Velocity is clipped to a user-defined maximum speed per agent v_{max} after this update. All steering behaviors are introduced to vector agents in a field-space.

Atop this foundation, we introduced three *dynamic* steering behaviors: pursuit (Figure 9), evasion, and wandering (Figure 10). Dynamic steering is proactive, allowing agents to anticipate the movement of other objects in their environment; this contrasts with static steering (see Reynolds, 1999, for example), which is simply reactive. For pursuit, an agent (p) identifies a moving target ($\vec{q}$) and tries to match its position to that target by acceleration ($\vec{a}$), dynamically and at its own user-defined maximum acceleration (a_{max}), as it shifts course. A pursuing agent knows the current position of the target; it calculates the time that it will take to reach that position and uses this as a prediction time ($\hat{t}$). If this time is very long (beyond a user-defined threshold), it is likely that the moving target will have changed its speed and heading remarkably

(i.e., while the agent was thinking about an intercept course, the object may be long-gone) and so we also provided a maximum prediction time (t_{max}) that was used to limit prediction error: if the prediction time is too long, the agent should use t_{max}.

$$\text{Direction of the target: } \vec{a} = \frac{\vec{q}-\vec{p}_o}{\vec{p}_t-\vec{p}_o} \cdot a_{max} \text{ , and}$$
$$\text{the future heading estimate: } \hat{t} = min\left(t_{max}, \frac{\vec{q}-\vec{p}}{v_{max}}\right), \text{ and } \hat{p} = \vec{p}_{\mathrm{t}} + \vec{v}_{\mathrm{t}} \cdot \hat{t} \quad \text{(vii)}$$

Evade behavior is the inverse of pursuit behavior.

[Figure 9 goes here.]

Wandering produces the steering equivalent of a random walk, with the difference that steering is constrained within a neighborhood. Although agents move randomly at each step; the constraint imposes some continuity in the agent's path at local scales. Operationally, this is achieved by casting a circular "attention zone" ahead of an agent (representing the local area in which its attention is focused). The radius (r_{wander}) and distance ($d_{wander_{offset}}$) of the zone are user-defined; changing their values alters the smoothness of the wandering. A random position on the circle is chosen and designated as a target ($\vec{q}$) for seek behavior. (This position can alternatively be specified by the size of a random deviation angle from the agent's moving direction.) Positioning on the attention zone is calculated as follows:

$$O_{wander'} = O_{wander} + \left(\text{random}(0,1) \cdot O_{wander_{max}}\right)$$

$$O_q = O_{wander'} + O_p \quad \text{(viii)}$$

$$\vec{q} = \vec{p} + \left(d_{wander_{offset}} \cdot O_p\right) + \left(r_{wander} \cdot O_q\right)$$

Above, O represents an agent's direction; $O_{wander'}$ is a subsequent wandering move following O_{wander}. The last line in equation (viii) requires conversion of agent orientation from radian (a scalar) to vector format in L, i.e., $(\cos\theta\,, \sin\theta)$, where θ is the angle in radians.

[Figure 10 goes here.]

3.10 Movement by social force

The social force model developed by Helbing and Molnár (1995) is popularly used to generate pedestrian motion in crowds. The model uses three forces: acceleration, attraction, and separation and these are chained using Langevin equations.

$$Acceleration = \vec{F}_p^0\left(\vec{v}_p, v_p^0 \vec{O}_p\right) \quad \text{(viv)}$$

$$Separation = \sum_q \vec{F}_{p,q}\left(\vec{O}_p, \vec{p} - \vec{q}\right) \quad \text{(x)}$$

$$Wall\ repulsion = \sum_W \vec{F}_{p,W}\left(\vec{O}_p, \vec{p} - \vec{p}_W\right) \quad \text{(xi)}$$

$$Attraction = \sum_i \vec{F}_{p,i}\left(\vec{O}_p, \vec{p} - \vec{\imath}, t\right) \quad \text{(xii)}$$

$$Motivation = (acceleration + separation + wall\,repulsion + \text{attraction}) + fluctuation \quad \text{(xiii)}$$

$\vec{F}$ denotes the force acting upon an agent's position ($\vec{p}$) at time zero [equation (viv)]; between an agent and target (q) tuple [equation (x)]; between an agent and a wall (W) [equation (xi)], and an agent and an attractor (i) [equation (xii)]. $\vec{v}_p$ indexes an agent's actual velocity, v_p its desired velocity, and $\vec{O}_p$ its desired heading. The fluctuation term in equation (xiii) introduces stochasticity.

[Figure 11 goes here.]

3.11 Movement by hopping

Movement by hopping is used to produce sudden relocation behavior. By hopping, an agent moves *instantaneously* to a random new location that has free space to accommodate it (Figure 12).

[Figure 12 goes here.]

3.12 Data collection and analysis

We collected a variety of real-world trajectory samples for different walker demographics, activities, environments, and scales to use as a comparison set (Table 2). With the exception of the play data reflected in Table 2, walkers' paths were recorded using Geographic Positioning Systems (GPS) enabled with wide-area augmentation systems and subjected to differential correction for increased positional accuracy. Play data were collected by human observers,

sketching the locations of individual children on a tablet PC, using customized GIS and on-screen digitizing software that we developed. (Data were collected in compliance with Institutional Review Board procedures for the protection of human subjects.) In total, 43.8 km of movement data was collected over 46 unique paths in five cities for our study.

[Table 2 goes here.]

Our models only consider movement of agents, so our focus in designing movement metrics was on capturing movement properties across four (related) domains: the correlation between successive turns in movement paths, the general level of turning over an entire path, relative path straightness, and movement fractality. Collectively, these allowed us to assess relative sinuosity of movement and to characterize the scale at which movement took place. We used Nams's (1996) VFractal measure to relate turning angle θ (considered between discrete consecutive steps in movement ($step$) that are fitted to a path with varying resolution) to the net length (Net) of step-pairs along a path for every step-and-turn tuple. This relationship (V) is calculated as follows (Nams, 1996).

$$V = \frac{\log(2)}{\log\left(\frac{Net}{step}\right)} = \frac{\theta}{1 + \log_2(\cos\theta + 1)} \quad \text{(ix)}$$

The mean cosine of turning angle ($\overline{\cos}\,\theta$) measures relative straightness over an *entire path* ($\overline{\cos}\,\theta = 1$ is straight). The correlation between successive turn angles ($corr\,\theta$) measures directional preservation on a *step-by-step* basis. We also calculated the fractal dimension (D) of

movement paths, using the standard divider method (Mandelbrot, 1977), to assess the ability of a path to fill a plane between one and two dimensions, where $D = 2$ denotes maximum sinuosity. Additionally, we calculated a mean fractal dimension ($\overline{D}$), which corrected for known overestimation errors in truncation when using the divider method at large scales (Nams, 2006).

[Table 2 goes here.]

4 Results

In order to investigate the relative performance of the movement algorithms described in the previous section, we first considered their correspondence with theory and the plausibility of their movement representations. Second, we compared them empirically and substantively to each other. Third, we examined the extent to which they might match recorded movements of people in the real-world. Because different movement routines are designed to operate at different scales, we will discuss the results with respect to macro-movement (urban-scale) and micro-movement (person-scale). (Note that several of the metrics we use cut *across* scales.)

4.1 Macro-movement

We built three distinct algorithms to drive macro-movement in simulation: movement by hopping, by hill-climbing, and by Dijkstra and A* shortest-path search. In each case, the algorithms were tested using a five-cell von Neumann and nine-cell Moore neighborhood, providing enough space for agents to examine the local space in their immediate vicinity.

4.1.1 Movement by hopping

Movement by hopping has little theoretical justification, save acknowledging that people may separate in space and time when moving, through cognitive dissonance (Sakoda, 1971), bias

(Clark and Fossett, 2008), or segregation (Schelling, 1969), for example. The hopping algorithm generated unrealistically high values of mean fractal dimension ($\overline{D} = 1.4398$) and at large scales ($scale \geq 35$), its VFractal tended toward a value of 2, i.e., it was *maximally sinuous* (Figure 13). This is significant as it shows that movement by hopping is random at macro-scales. Directional correlation among successive steps was strongly negative ($corr\ \theta = -0.514$) (Appendix 1). The entire picture is unrealistic, suggesting random movement in every facet of the path. People almost never move randomly at macro-scales; in an urban context, pedestrian walkers are almost always going *somewhere* meaningful, usually with serial autocorrelation in the movements that they take to get there. Movement by hopping is not particularly useful as a proxy for pedestrian movement. This is perhaps obvious, but it is useful to demonstrate this quantitatively, particularly because hopping is used in computational social science models (see Epstein, 2002, for example).

[Figure 13 goes here.]

4.1.2 Movement by path-planning

Movement by path-planning has a reasonably sound theoretical justification. Path-planning is associated with human way-finding, because walkers segment their trips hierarchically and move between space-time waypoints (Raubal and Egenhofer, 1998). Path-planning is also related to spatial cognition, because walkers generally rely on a mental map of the environment through which they intend to traverse (Golledge, 1999) and they commonly use a minimization heuristic for way-finding. Over an entire trip, for example, pedestrians generally adopt a course from origin to destination that is close to the shortest path between those points (Ciolek, 1981). This behavior has been observed in downtown environments (Gärling and Gärling, 1988) and

shopping malls (Zacharias, 2001). There is also a real-world analog for encoding movement paths in a graph structure, because urban pedestrians walk along sidewalks, which usually follow a gridded, connected, network layout (Zacharias, 2001) and there exists evidence that pedestrians imagine their environment metrically when walking (Vishton and Cutting, 1995). The A* algorithm, in particular, is well-supported in theory because walkers' knowledge of waypoints along a path may be most accurate for origin and destinations (compared to the places in between), particularly when origins and destinations present as home or work locations, or as landmarks such as transport hubs, retail sites, and entertainment venues (Foltête and Piombini, 2007).

Measures of mean fractal dimension for movement by path-planning, across all heuristics, were lower than those generated by hopping ($1.0833 \leq \overline{D} \leq 1.1936$ for path-planning, compared to $\overline{D} = 1.4398$ for hopping). They were, in other words, more "reasonable". However, based on our metrics, all of the paths generated by path-planning were a poor match to real-world data. For example, we collected data for pedestrian movement through a relatively non-crowded downtown streetscape in Salt Lake City, UT (Figure 14). Simulated path-planning produced little turning at a macro-scale and this was a close match to the observed data ($\overline{\cos}\,\theta = 0.923$ for the Salt Lake City example, versus $\overline{\cos}\,\theta \sim 0.93$ for the path-planning algorithms). This is perhaps understandable given the geometry of the street network in which walking took place in both examples. However, differences presented at the scale of the *sub-path* (i.e., movement within-the-path), where movement in simulation was more sinuous than was observed in the real-world ($1.178 \leq \overline{D} \leq 1.1936$ for the simulations, versus $\overline{D} = 1.0295$ for the Salt Lake City example). This may be because the simulation algorithms produced a lot of lateral movement and

zigzagging at local scales, i.e., the path that they produced was relatively straight at a macro-level, but not at a micro-level (compare Figures 4, 5, and 14); pedestrians in the real-world often like to preserve the *straightest* path along their trip (Hillier and Hanson, 1984).

This finding is significant because it suggests that path-planning algorithms might be useful as a *global* movement scheme, but a different algorithm may be required to produce realistic *local* movement. The path-planning heuristics were run for nine-cell Moore and five-cell von Neumann neighborhoods. In each case, the value of $\overline{D}$ was slightly higher for the von Neumann filter. The difference in $\overline{D}$ between the filters is small, but this may indicate that the "*bandwidth*" of information available to agents might influence their movement. The von Neumann filter presents agents with a smaller *volume of information* than the Moore case and this may cause agents to move into less-than-optimal positions relative to the shortest path, thereby creating added sinuosity. The von Neumann filter also presents agents with fewer movement *options* (four, compared to the Moore filter's eight) and agents may therefore find relative difficulty in preserving straight lines while also trying to satisfy the algorithm's shortest-path heuristic.

[Figure 14 goes here.]

4.2 Micro-movement

Eight algorithms for local movement were constructed and run in simulation: movement by steering (wandering, dynamic seeking, dynamic fleeing), by greedy hill-climbing, by Brownian motion, by Lévy flight, by random walk, and by social force. Movement by greedy hill-search was run for five-cell von Neumann neighborhoods and nine-cell Moore neighborhoods. Brownian motion, Lévy flight, and random walks were run over three durations: short- (4,590 time-steps), medium- (10,031 time-steps), and long-range (37,188 time-steps). These algorithms

are considered *micro* because they operate only on conditions that agents perceive in their vicinity, rather than incorporating the sorts of global information that the path-planning routines made use of (origin-destination, path preservation heuristics, global graph and metric distance-to-destination).

4.2.1 Movement by random-walk

The theoretical justification for pedestrian random walks comes from analogies between the behavior of pedestrians in densely-packed crowds and the dynamics of particles in physical flows (Henderson, 1971), whereby it is assumed that pedestrian crowds will behave as excitable media when in extreme situations (Farkas et al., 2002; Schweitzer, 2003). Similar signatures of complexity, such as spontaneous lane formation (Blue and Adler, 2001), annealing (Helbing et al., 2001), striping (Helbing, 1992), and freezing by heating (Stanley, 2000) have been hypothesized as manifesting in crowd and particle flows and this is often used as justification for the application of physical equations to the modeling of pedestrian movement (Henein and White, 2007). The physical rationale for pedestrian behavior is at odds with behavioral explanations, from sociology (Couch, 1968), psychiatry (Mawson, 2005), and safety management (Bohannan, 2005), however, which suggest that the interactive relationships between pedestrians are much more complicated than those expressed in particle-based models. Observations from crowd safety studies, for example, highlight that people do not behave like dumb, excited particles in extreme settings and that they are often very *humane* in their interactions (Couch, 1968; Pauls, 1984).

The results for simple random walks were far more sinuous than any of the real-world data collected. In the case of long-range random walks, the paths approached the maximum potential tortuousity ($\overline{D} = 1.9252$).

In contrast, walks generated by Brownian motion generated a level of sinuosity that was comparable to real-world data in some instances. We recorded values of $\overline{D} = 1.1085$, $\overline{D} = 1.224$, and $\overline{D} = 1.261$ for short-range, medium-range, and long-range Brownian trips respectively. Brownian motion over *short ranges* actually produced reasonable movement paths ($\overline{D} = 1.1085$). Across all scales, Brownian motion also provided a good analog for *very dense crowds*: the values compared well with the extremes of high-density movement of real pedestrians over Tokyo's Shibuya crossing, for which values of $1.0876 \leq \overline{D} \leq 1.2629$ were recorded (although, trips over this crosswalk are relatively short in reality). Similarly, the match to values for Yokohama (on a retail high street, where sidewalks are often quite full) were good ($1.1037 \leq \overline{D} \leq 1.184$). Lévy-flight walks also generated reasonable paths ($1.1085 \leq \overline{D} \leq 1.1309$), but did so at all scales.

These results suggest that, at local scales and in very high density crowds, pedestrian walking may be close to Brownian motion in the geometry of the paths that it produces (the Shibuya crossing is one of the world's busiest crossings). In these cases, pedestrians may engage in many rapid, small course adjustments to avoid collisions or to correct their path under the influence of many potential interactions. This was apparent in the VFractal profile for the Shibuya data, for example. The value of *V* was much higher at local-scales than at macro-scales (Figure 15). The Lévy flight, which scales long, straight movement relative to short, tortuous movement seems particularly well-suited to generating paths that ally with real-world human motion in dense

urban settings (such as Yokohama). This makes sense: pedestrian movement along urban streetscapes in downtown settings, such as the spaces that we sampled in Japan, could reasonably be considered as involving short-lived periods of free-walking, punctuated more frequently by the need to avoid collisions in relatively smaller movements.

[Figure 15 goes here.]

The real-world movement samples from the pre-school center also have a potentially close analogy with random walks (children are, after all, a particularly excitable human medium). Movement through festival crowds is another appropriate analog, as pedestrians in those settings may well be wandering to browse or move subject to a larger crowd flow without a predictable course. However, none of the random walk behaviors was a good match to the pre-school data or the festival data (Appendix 1).

4.2.2 Movement by greedy hill-climbing

We considered greedy hill-climbing as a micro-movement scheme because of its relationship to information-gathering and movement in cellular automata pedestrian models. Movement by hill-climbing has some theoretical justification. Goffman (1971), for example, outlined the procedure by which pedestrian walkers search for collisions by scanning their environment in a small circle around them, ignoring features at a distance. Although the movement metrics produced by hill-climbing were a reasonable match for much of the real-world data that we collected (Appendix 1), the algorithm failed to resolve a path in our tests, even in a relatively straightforward synthetic urban environment (Figure 3). It would only work over short distances in relatively open environments, becoming otherwise mired in local maxima or minima. Without the added macro-guidance that was included in the Dijkstra and A* heuristics, the hill-climbing routine has

no way to resolve these conflicts. (Similar results were reported in Haklay *et al.* (2001), where a "helmsman" module had to be introduced to "wiggle" agents free of such minima/maxima; the number of instances of wiggling were not reported.) The widespread use of hill-climbing as a proxy for movement in cellular automata pedestrian models (see models by Batty, 2003, which are purposely abstract in this way) therefore seems questionable.

Our findings for greedy hill-climbing ally with conventional theory regarding behavioral geography, which suggests that people navigate and move with *both* local and global information and motivations (Golledge, 1999). (It may be difficult to achieve action-by-proximity *and* action-at-a-distance using cellular automata models, however.) Recall also that we used relatively small-area neighborhood filters (five- and nine-cell, as is commonly the case in most cellular pedestrian models; see Torrens (2005) for an overview). It is possible that better thought-out vision filters could overcome the entrapment problem. There is some debate, for example, about the size (and shape) that vision filters should use. Space syntax approaches characterize vision in terms of "axial" lines-of-sight (Penn, 2003; Turner and Penn, 2002), for example, that relate vision to the geometry (axes) of the built infrastructure through which people proceed. Wolff (1973) observed that walkers used up to a 30m threshold for assessing their next step in low density situations, but that they constrained that filter to 1.5m in high density conditions. Using eye-tracking technologies, Kitazawa and Fujiyama (2010) estimated the distance to be just a few meters (for which a Moore or von Neumann neighborhood of nine or five "person-sized" cells would seem plausible).

4.2.3 Movement by steering

The theoretical justification for movement by steering is varied. People steer to escape collisions (Cutting et al., 1995) and to avail of interactions (Whyte, 1980). The magnitude of steering is also relevant Wang and Cutting (1999) noted people's tendency to steer in a narrow region of interaction and Dabbs and Stokes (1975) described how walkers yielded wider berth when avoiding groups of pedestrians than when avoiding individuals.

We collected trajectory samples from an art festival in an American downtown and a zoo festival. Because of the need for pedestrians to avoid other members of the crowd, to wander when browsing sights, or to seek out attractions in these events, we considered them to be a good analog for steering. The children's movement data we described previously are also a good comparison set because paths were sampled in a pre-school where children engaged in games of racing, baseball, pretending to be animals, and so on, which involved short bursts of seeking and fleeing.

The values of fractal mean were $\overline{D} = 1.1951$ for the art festival and $1.0743 \leq \overline{D} \leq 1.2062$ for the zoo festival (Appendix 1). Correlations among successive turns were close to zero in all but two of the festival paths. Moreover, the mean cosine of turning angles over the entire path was $0.19 \leq \overline{\cos}\,\theta \leq 0.731$ for both sets of festival data. This indicates a lack of directional preservation in the festival data, at scales from the local to the global. These festival data were not a good match to the simulated paths produced by steering, likely because the real-world data was collected for individual paths in a large and dense crowd (thousands of people in the case of the zoo festival), but our simulations in this case took place without crowds.

For toddler movement in the pre-school sample, $\overline{D}$ was relatively low (among the lowest values recorded through all of our real-world sampling): $1.0169 \leq \overline{D} \leq 1.1617$, with a relatively strong negative correlation between successive turn angles ($-0.636 \leq corr\ \theta \leq -0.392$). This suggests relatively uncoordinated movement. The values for simulated movement by steering were lower than those for the pre-school sample, but they were the closest match. It would seem that steering at a local scale cannot independently generate movement with an analog in the real-world paths we observed. Once again, these findings point to a conclusion that *many* movement schemes are needed, in parallel, to generate realistic-seeming paths through space and time.

4.2.4 Movement by social force

We tested the social force model on a simulation of many-interacting pedestrians in a dense crowd, using social forces to move agents and a bounding wall to encapsulate them [wall repulsion is part of the original model, see equation (xi); the space was treated as toroidal, so that agents moving over one edge would reappear on the opposite side with continuity] (Figure 11). The model produced paths with $1.1152 \leq \overline{D} \leq 1.3427$. The correlation among successive turn angles was the highest of all scenarios we considered (Appendix 1) ($corr\ \theta \sim 1$). While some of the paths generated by social force were consistent with real-world data for very high density situations (extreme sinuosity over the Shibuya crossing, for example), the amount of sinuosity produced in simulation was considerably higher than more quotidian examples of movement. For example, the modeled paths did not compare favorably with real-world paths for walking in low-density crowds on a university campus ($\overline{D} = 1.0441$) or through an open-air shopping mall ($\overline{D} = 1.0515$). Measures of fractal mean did compare well with the festival data, but only for the lower-range of $\overline{D}$ for social force movement. Notably, the social force model produced many

artifacts in simulation: agents moving backwards to avoid collision and frequent compound retreating due to sequences of near-collision that prompted them to take many steps backwards in order to move forward (this is evident in the colored traces of movement shown in Figure 11). Pedestrians ordinarily prefer to travel in a direction that faces their destination (Hillier and Hanson, 1984). Normally, they will not orient themselves in directions that oppose the direction of their goal (Older, 1968) and common knowledge suggests that they will rarely perform about-face maneuvers when they are already mobile. While the force analogy may be useful for the flow of an *entire crowd mass* or for *very dense crowds*, it does not seem appropriate for simulating individual movement paths in quotidian scenarios.

5 Conclusions

In this paper, we examined popular algorithms as motion controllers for synthetic pedestrians in agent-based models, with the intention of assessing whether they faithfully represent real-world movement. This required development of an extensible agent-based modeling platform that could represent varying movement schemes, as well as a suite of analytical tools that could relate simulated movement between models and relative to real-world pedestrian trajectories.

The *modeling scheme* that we introduced, based on geographic automata, proved efficient in representing a diverse range of movement schemes. Indeed, all of the models that we tested were accommodated using geographic automata. The approach has some distinct advantages in representing multiple spaces in simulation and facilitating their cross-interaction. Our *analysis scheme* also proved useful, in benchmarking diverse movements across different scales. The utility of the analysis could clearly be extended by "docking" additional metrics—measures of

complexity (Batty and Torrens, 2005), sociometrics (Waaserman and Faust, 1994), or time geography (Miller and Bridwell, 2009) may add further context.

Some algorithms do not seem to function as productive proxies for pedestrian movement. This includes movement by hopping and simple random walk. Understandably, these are among the *most* abstract of movement regimes, but they are still used to generate agent mobility in pedestrian (Batty, 2003; Batty et al., 2003b) and computational social science models (Epstein, 2002), including applications where movement is characterized as particularly significant (Gorman et al., 2006). These techniques are prevalent in agent-based disease transmission models (Epstein et al., 2008), even where such models are advertised as being spatially explicit (Eggo et al., 2010) and despite general agreement that disease dynamics are linked to mobility of host and vector agents (Ferguson et al., 2006; Hess, 1996), as well as the movement of disease events such as epidemics or pandemics (Grenfell et al., 2001). The treatment of movement in disease transmission models was understood to be problematic almost four decades ago [see Noble (1974)], but relatively little has been done to remedy the problem.

Other algorithms have reasonably sound theoretical foundation and perform well at particular scales, but not others. Path-planning, for example, is relatively appropriate for global movement, but not for local movement.

There are also algorithms that have relatively little theoretical justification, but perform reasonably well against real-world data: Brownian motion is an example. Such algorithms are difficult to use in simulations used to support theory or decisions because they fundamentally do not match real-world behavior. They do, however, have usefulness, for example, in ascribing stochasticity to movement generated by other, theoretically-plausible, behavior.

We also found that some movement schemes, while theoretically plausible, are problematic simulators for movement. The often-used greedy search heuristic is an example. The algorithm represents pedestrians' tendency to scan their immediate environment and react to information on a step-by-step basis. However, it failed to resolve paths through anything but the most simple environments, largely because it did not consider other, related, movement processes operating at different scales (global path-planning) or information beyond the micro-scale. Similarly, steering (which is perhaps the best fit to behavioral geography of all of the methods we examined) could not generate realistic movement when used exclusively as a motion controller. Social force models are also suitable for specific contexts (high density crowds in confined spaces) but do not work well in isolation.

Lévy flights are an exception of sorts: they performed relatively well in simulation, capturing elements of movement across scales. Interestingly, correlation of movement across scales follows a power-law distribution in Lévy flights, which matches recent evidence that trip-making at population levels follows high-magnitude/low-frequency distributions (Brockman et al., 2006; González et al., 2008), rather than the fractal relationship that is found in many particle-based physical systems that are often compared to pedestrian flows.

In summary, our results suggest that *all* of the mechanisms responsible for pedestrian movement should be treated in an integrated fashion in simulation and that careful attention should be paid to relating algorithms to their characteristic scales, as well as providing opportunities for emergence across scales through appropriate (behaviorally-plausible) mechanisms. Clearly, *information*—as well as how agents acquire that information, how they process it relative to their evolving mental maps, how they interpret their findings relative to the often partial

understanding they have of their ambient environment, and how they translate information into movement—plays an important role in this regard. Our analysis demonstrated the significance of simply adapting neighborhood filters for mobile agents. While some proxy representations of movement are "good enough" to generate mobility in simulation, the field would perhaps benefit from further exploration into mechanisms of behavioral geography that drive movement in the real-world: how movement behaviors interact; how they scale; and how they relate to the social, built, and technical environment of today's cities. This requires careful consideration of how those behaviors might best be translated in into computable form for agent-based modeling and schemes for assessing the validity of that translation.

6 References

Allbeck J, Kipper K, Adams C, Schuler W, Zoubanova E, Badler N, Palmer M, Joshi A, 2002, "ACUMEN: amplifying control and understanding of multiple entities", in *The First International Joint Conference on Autonomous Agents and Multiagent Systems*, ACM, Bologna, Italy pp 191-198

Bartumeus F, da Luz M G E, Viswanathan G M, Catalan J, 2005, "Animal search strategies: a quantitative random-walk analysis" *Ecology* **86** 3078-3087

Batty M, 2003, "Agent-based pedestrian modelling", in *Advanced Spatial Analysis: The CASA Book of GIS* Eds P A Longley, M Batty (ESRI Press, Redlands) pp 81-107

Batty M, Desyllas J, Duxbury E, 2003a, "The discrete dynamics of small-scale spatial events: Agent-based models of mobility in carnivals and street parades" *International Journal of Geographical Information Science* **17** 673-697

Batty M, Desyllas J, Duxbury E, 2003b, "Safety in numbers? Modelling crowds and designing control for the Notting Hill carnival" *Urban Studies* **40** 1573-1590

Batty M, Torrens P M, 2005, "Modeling and prediction in a complex world" *Futures* **37** 745-766

Blue V, Adler J, 2001, "Cellular automata microsimulation for modeling bi-directional pedestrian walkways" *Transportation Research Part B* **35** 293-312

Bohannan J, 2005, "Directing the herd: crowds and the science of evacuation" *Science* **310** 219-221

Boulic R, Noser H, Thalmann D, 1994, "Automatic derivation of curved human walking trajectories from synthetic vision", in *Computer Animation '94*, Geneva, Switzerland pp 93-103

Brockman D, Hufnagel L, Geisel T, 2006, "The scaling laws of human travel" *Nature* **439** 462-465

Chenney S, 2004, "Flow tiles", in *Proceedings of the 2004 ACM SIGGRAPH/Eurographics symposium on Computer Animation*, Aire-la-Ville, Switzerland pp 233-242

Ciolek T M, 1981, "Pedestrian behaviour in pedestrian spaces: some findings of a naturalistic field study", in *Understanding The Built Environment - Proceedings of he Annual Conference of the ANZAScA* Ed S V Szokolay (Australian and New Zealand Architectural Science Association, Canberra) pp 95-112

Clark W A V, Fossett M, 2008, "Understanding the social context of the Schelling segregation model" *Proceedings of the National Academy of Sciences* **105** 4109-4114

Couch C, 1968, "Collective behavior: An examination of some stereotypes" *Social Problems* **15** 310-322

Crooks A, Hudson-Smith A, Dearden J, 2009, "Agent Street: an environment for exploring agent-based models in Second Life" *Journal of Artificial Societies and Social Simulation* **12** 10 (Online)

Cutting J E, Vishton P M, Braren P A, 1995, "How we avoid collisions with staionary and moving obstacles" *Psychological Review* **102** 627-651

Dabbs J M, Stokes III N A, 1975, "Beauty is power: the use of space on the sidewalk" *Sociometry* **38** 551-557

Dijkstra E W, 1959, "A note on two problems in connection with graphs" *Numerische Mathematik* **1** 269-271

Dodge S, Weibel R, Forootan E, 2009, "Revealing the physics of movement: Comparing the similarity of movement characteristics of different types of moving objects" *Computers, Environment and Urban Systems* **33** 419-434

Eggo R M, Cauchemez S, Ferguson N M, 2010, "Spatial dynamics of the 1918 influenza pandemic in England, Wales and the United States" *Journal of The Royal Society Interface* forthcoming

Epstein J M, 2002, "Modeling civil violence: an agent-based computational approach" *Proceedings of the National Academy of Science* **99** 7243-7250

Epstein J M, Parker J, Cummings D, Hammond R A, 2008, "Coupled contagion dynamics of fear and disease: mathematical and computational explorations" *PLoS ONE* **3** e3955

Farkas I, Helbing D, Vicsek T, 2002, "Crowd behaves as excitable media during Mexican wave" *Nature* **419** 131

Ferguson N M, Cummings D A T, Fraser C, Cajka J C, Cooley P C, Burke D S, 2006, "Strategies for mitigating an influenza pandemic" *Nature* **442** 448-452

Foltête J-C, Piombini A, 2007, "Urban layout, landscape features and pedestrian usage" *Landscape and Urban Planning* **81** 225-234

Fruin J J, 1971 *Pedestrian Planning and Design* (Metropolitan Association of Urban Designers and Environmental Planners, Inc., New York)

Gärling T, Gärling E, 1988, "Distance minimization in downtown pedestrian shopping" *Environment and Planning A* **20** 547-554

Gipps P G, Marksjö B, 1985, "A microsimulation model for pedestrian flows" *Mathemathics and Computers in Simulation* **27** 95-105

Goffmann E, 1971 *Relations in Public: Microstudies in the Public Order* (Basic Books, New York)

Golledge R A, 1999 *Wayfinding Behavior: Cognitive Mapping and Other Spatial Processes* (The Johns Hopkins Press, Baltimore)

González M C, Hidalgo C A, Barabási A-L, 2008, "Understanding individual human mobility patterns" *Nature* **453** 779-782

Gorman D M, Mezic J, Mezic I, Gruenewald P J, 2006, "Agent-based modeling of drinking behavior: a preliminary model and potential applications to theory and practice" *American Journal of Public Health* **96** 2055-2060

Grenfell B T, Bjørnstad O N, Kappey J, 2001, "Travelling waves and spatial hierarchies in measles epidemics" *Nature* **414** 716-723

Guy S J, Chhugani J, Curtis S, Dubey P, Lin M, Manocha D, 2010, "PLEdestrians: a least-effort approach to crowd simulation", in *Eurographics/ACM SIGGRAPH Symposium on Computer Animation* Eds M Otaduy, Z Popović (Association of Computer Machinery, Madrid)

Haklay M, O'Sullivan D, Thurstain-Goodwin M, Schelhorn T, 2001, ""So go downtown": simulating pedestrian movement in town centres" *Environment and Planning B* **28** 343-359

Hart P E, Nilsson N J, Raphael B, 1968, "A formal basis for the heuristic determination of minimum cost paths" *IEEE Transactions on Systems Science and Cybernetics* **4** 100-107

Helbing D, 1992, "A fluid-dynamic model for the movement of pedestrians" *Complex Systems* **6** 391-415

Helbing D, Molnár P, 1995, "Social force model for pedestrian dynamics" *Physical Review E* **51** 4282-4286

Helbing D, Molnár P, 1997, "Self-organization phenomena in pedestrian crowds", in *Self-organization of Complex Structures: From Individual to Collective Dynamics* Ed F Schweitzer (Gordon and Breach, London) pp 569-577

Helbing D, Molnár P, Farkas I, Bolay K, 2001, "Self-organizing pedestrian movement" *Environment and Planning B* **28** 361-383

Henderson L F, 1971, "The statistics of crowd fluids" *Nature* **229** 381-383

Henein C M, White T, 2007, "Macroscopic effects of microscopic forces between agents in crowd models" *Physica A* **373** 694-712

Hess G, 1996, "Disease in metapopulation models: implications for conservation" *Ecology* **77** 1617-1632

Hillier B, Hanson J, 1984 *The Social Logic of Space* (Cambridge University Press, Cambridge)

Hoogendoorn S P, Bovy P H L, 2000, "Gas-kinetic modeling and simulation of pedestrian flows" *Transportation Research Record* **1710** 28-36

Hoogendoorn S P, Daamen W, 2005, "Pedestrian behavior at bottlenecks" *Transportation Science* **39** 147-159

Hughes R L, 2003, "The flow of human crowds" *Annual Review of Fluid Mechanics* **35** 169-182

Jiang B, Jia T, 2009, "Studying spatial effects on human mobility patterns using agent-based simulations", in *Tenth International Conference on Geocomputation* Eds B G Lees, S W Laffan (University of New South Wales, Sydney)

Jiang B, Yin J, Zhao S, 2009, "Characterizing human mobility patterns in a large street network" *Physical Review E* **80** 021136

Johansson A, Helbing D, Al-Abideen H, Al-Bosta S, 2008, "From crowd dynamics to crowd safety: a video-based analysis" *Advances in Complex Systems* **11** 497-527

Keßel A, Klüpfel H, Schreckenberg M, 2002, "Microscopic simulation of pedestrian crowd motion", in *Pedestrian and Evacuation Dynamics* Eds M Schreckenberg, S D Sharma (Springer, Berlin)

Kitazawa K, Fujiyama T, 2010, "Pedestrian vision and collision avoidance behavior: investigation of the information process space of pedestrians using an eye tracker", in *Pedestrian and Evacuation Dynamics 2008* Eds W W F Klingsch, C Rogsch, A Schadschneider, M Schreckenberg (Springer, Berlin) pp 95-108

Kukla R, Kerridge J, Willis A, Hine J, 2001, "PEDFLOW: development of an autonomous agent model of pedestrian flow" *Transportation Research Record: Journal of the Transportation Research Board* **1774** 11-17

Lee K H, Choi M G, Hong Q, Lee J, 2007, "Group behavior from video: a data-driven approach to crowd simulation", in *2007 ACM SIGGRAPH/Eurographics symposium on Computer animation* Eds M Gleicher, D Thalmann (Eurographics Association, San Diego, California)

Lerner A, Chrysanthou Y, Lischinski D, 2007, "Crowds by Example" *Computer Graphics Forum* **26** 655-664

Lormen T H, Leiserson C E, Rivest R L, Stein C, 2007 *Introduction to Algorithms* (MIT Press, Cambridge, MA)

Mandelbrot B, 1977 *The Fractal Geometry of Nature* (W.H. Freeman, San Francisco)

Mawson A R, 2005, "Understanding mass panic and other collective responses to threat and disaster" *Psychiatry: Interpersonal & Biological Processes* **68** 95-113

Miller H J, Bridwell S A, 2009, "A field-based theory for time geography" *Annals of the Association of American Geographers* **99** 49-75

Moussaïd M, Helbing D, Garnier S, Johansson A, Combe M, Theraulaz G, 2009, "Experimental study of the behavioural mechanisms underlying self-organization in human crowds" *Proceedings of the Royal Society B: Biological Sciences* **276** 2755-2762

Musse S R, Thalmann D, 1997, "A model of human crowd behavior: group inter-relationship and collision detection analysis", in *Computer Animation and Simulations '97, Proceedings of the Eurographics Workshop, September 4-8* Eds I Herman, G Krammer (Budapest: Springer-Verlag) pp 39-51

Nagatani T, Nagai R, 2004, "Statistical characteristics of evacuation without visibility in random walk model" *Physica A: Statistical Mechanics and its Applications* **341** 638-648

Nams V O, 1996, "The VFractal: a new estimator for fractal dimension of animal movement paths" *Landscape Ecology* **11** 289-297

Nams V O, 2006, "Improving accuracy and precision in estimating fractal dimension of animal movement paths" *Acta Biotheoretica* **54** 1-11

Nara A, Torrens P M, 2007, "Spatial and temporal analysis of pedestrian egress behavior and efficiency", in *Association of Computing Machinery (ACM) Advances in Geographic Information Systems* Eds H Samet, C Shahabi, M Schneider (Association of Computing Machinery, New York) pp 284-287

Newton I, 1687 *Philosophiae Naturalis Principia Mathematica* (Royal Society of London for the Improvement of Natural Knowledge, London)

Nieuwenhuisen D, Kamphuis A, Overmars M H, 2007, "High quality navigation in computer games" *Science of Computer Programming* **67** 91-104

Noble J V, 1974, "Geographic and temporal development of plagues" *Nature* **250** 726-729

Older S, 1968, "Movement of pedestrians on footways in shopping streets" *Traffic Engineering and Control* **10** 160-163

Patil S, van den Berg J, Curtis S, Lin M C, Manocha D, 2010, "Directing crowd simulations using navigation fields" *IEEE Transactions on Visualization and Computer Graphics* **(to appear)**

Pauls J, 1984, "The movement of people in buildings and design solutions for means of egress" *Fire Technology* **20** 27-47

Pelechano N, Allbeck J, Badler N I, 2008 *Virtual Crowds: Methods, Simulation, and Control* (Morgan & Claypool, San Rafael, CA)

Penn A, 2003, "Space syntax and spatial cognition: or why the axial line?" *Environment and Behavior* **35** 30-65

Raubal M, Egenhofer M J, 1998, "Comparing the complexity of wayfinding tasks in built environments" *Environment and Planning B: Planning and Design* **25** 895-913

Renault O, Magnenat-Thalmann N, Thalmann D, 1990, "A vision-based approach to behavioral animation" *The Journal of Visualization and Computer Animation* **1** 18-21

Reynolds C W, 1987, "Flocks, herds, and schools: A distributed behavioral model" *Computer Graphics* **21** 25-34

Reynolds C W, 1999, "Steering behaviors for autonomous characters", in *Proceedings of the Game Developers Conference, 1999* Ed Game Developers Conference (Miller Freeman Game Group, San Jose, CA) pp 763-782

Reznor T, 2005, "All the love in the world", (Leaving Hope Music/TVT Music (ASCAP))

Russell S, Norvig P, 1995 *Artificial Intelligence: A Modern Approach* (Prentice-Hall, Upper Saddle River, New Jersey)

Sakoda J M, 1971, "The checkerboard model of social interaction" *Journal of Mathematical Sociology* **1** 119-132

Sakuma T, Mukai T, Kuriyama S, 2005, "Psychological model for animating crowded pedestrians" *Computer Animation and Virtual Worlds* **16** 343-351

Schelling T C, 1969, "Models of segregation" *American Economic Review* **59** 488-493

Schweitzer F, 1997, "Active brownian particles: Artificial agents in physics", in *Stochastic Dynamics* Eds T Pöschel, L Schimansky-Geier (Springer-Verlag, Berlin) pp 358-371

Schweitzer F, 2003 *Brownian Agents and Active Particles* (Springer-Verlag, Berlin)

Singh S, Kapadia M, Faloutsos P, Reinman G, 2009, "SteerBench: a benchmark suite for evaluating steering behaviors" *Computer Animation and Virtual Worlds* **20** 533-548

Stanley H E, 2000, "Non-equilibrium physics: Freezing by heating" *Nature* **404** 718-719

Tecchia F, Loscos C, Chrysanthou Y, 2002, "Visualizing crowds in real-time" *Computer Graphics Forum* **21** 753-765

Torrens P M, 2005, "Geosimulation approaches to traffic modeling", in *Transport Geography and Spatial Systems* Eds P Stopher, K Button, K Haynes, D Hensher (Pergamon, London) pp 549-565

Torrens P M, Benenson I, 2005, "Geographic Automata Systems" *International Journal of Geographical Information Science* **19** 385-412

Treuille A, Cooper S, Popović Z, 2006, "Continuum Crowds" *ACM Transactions on Graphics* **25** 1160-1168

Turing A M, 1950, "Computing machinery and intelligence" *Mind* **49** 433-460

Turner A, Penn A, 2002, "Encoding natural movement as an agent-based system: an investigation into human pedestrian behaviour in the built environment" *Environment and Planning B: Planning and Design* **29** 473 - 490

Venuti F, Bruno L, Bellomo N, 2007, "Crowd dynamics on a moving platform: mathematical modelling and application to lively footbridges" *Mathematical and Computer Modelling* **45** 252-269

Vicsek T, 2003, "Crowd control" *Europhysics News* **34** 45-49

Vishton P M, Cutting J E, 1995, "Wayfinding, displacements, and mental maps: velocity fields are not typically used to determine one's aimpoint" *Journal of Experimental Psychology* **21** 978-995

Waaserman S, Faust K, 1994 *Social Network Analysis: Methods and Applications* (Cambridge University Press, Cambridge)

Wang R F, Cutting J E, 1999, "Where we go with a little good information" *Psychological Science* **10** 71-75

Watkinson J, 2002 *An Introduction to Digital Audio* (Focal Press, Oxford)

Whyte W H, 1980 *The Social Life of Small Urban Spaces* (The Conservation Foundation, Washington D.C.)

Wolff M, 1973, "Notes on the behavior of pedestrians", in *People in Places: The Sociology of the Familiar* Eds A Birenbaum, E Sagarin (Praeger, New York) pp 35-48

Zacharias J, 2001, "Pedestrian behavior and perception in urban walking environments" *Journal of Planning Literature* **16** 3-18

Zhang Q, 2009, "Simulated annealing and crowd dynamics: approaches for intelligent control", in *Advances in Intelligent and Soft Computing 56: The Sixth International Symposium on Neural Networks* Eds H Wang, Y Shen, T Huang, Z Zeng (Springer, Berlin) pp 501-506

Figures

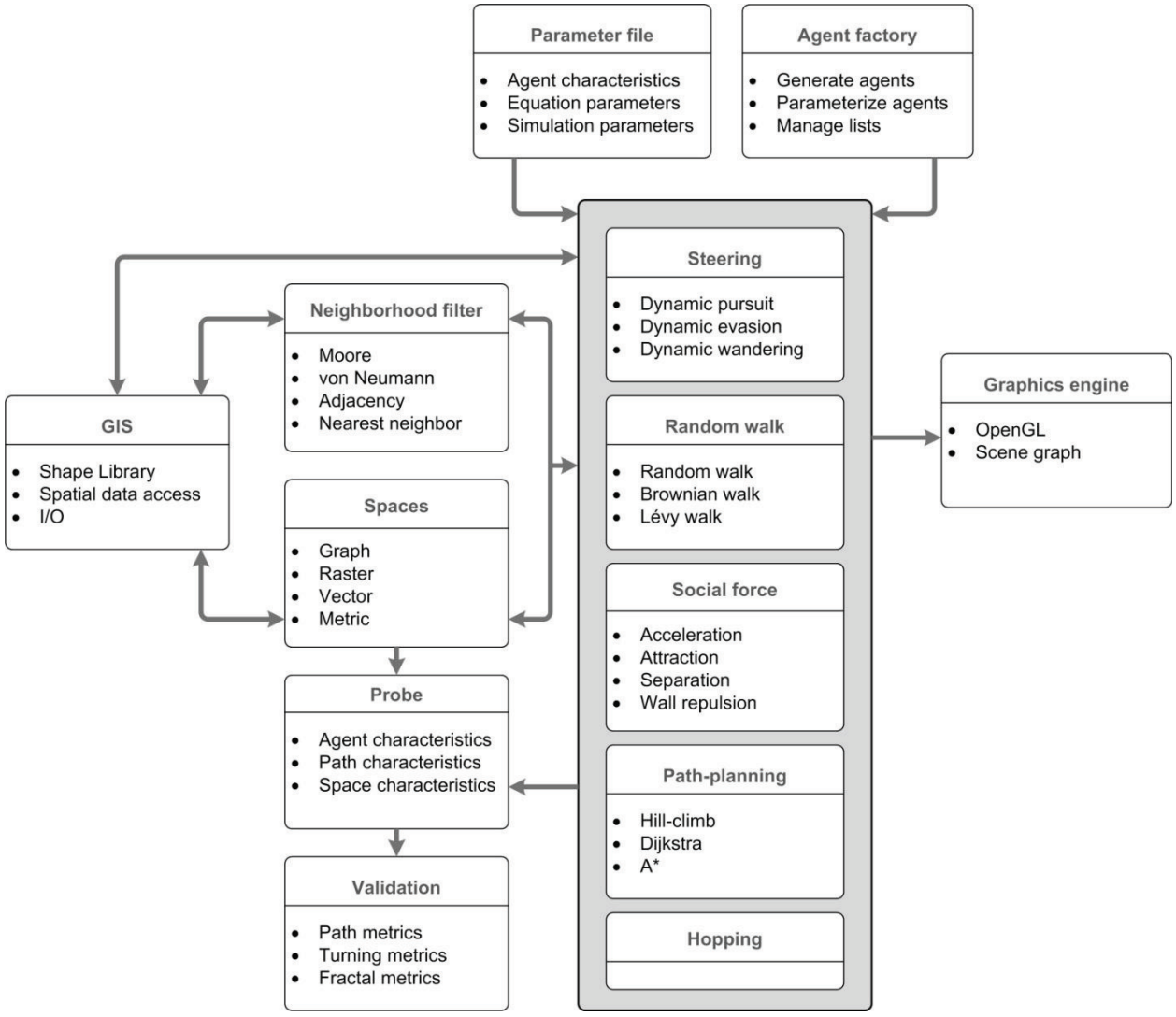

Figure 1. An overview of the main software modules that run the simulations.

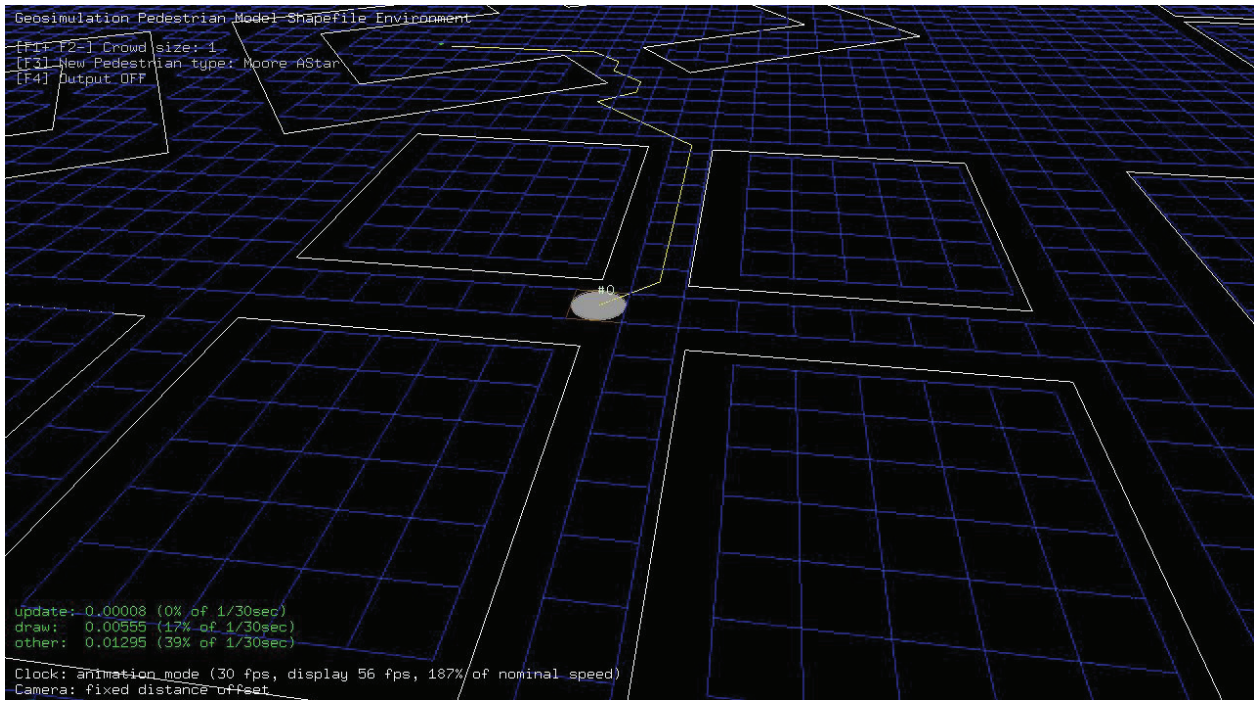

Figure 2. A view of simulation running on-screen; objects in the model may be queried by clicking during run-time and the data will be dynamically drawn from the underlying GIS.

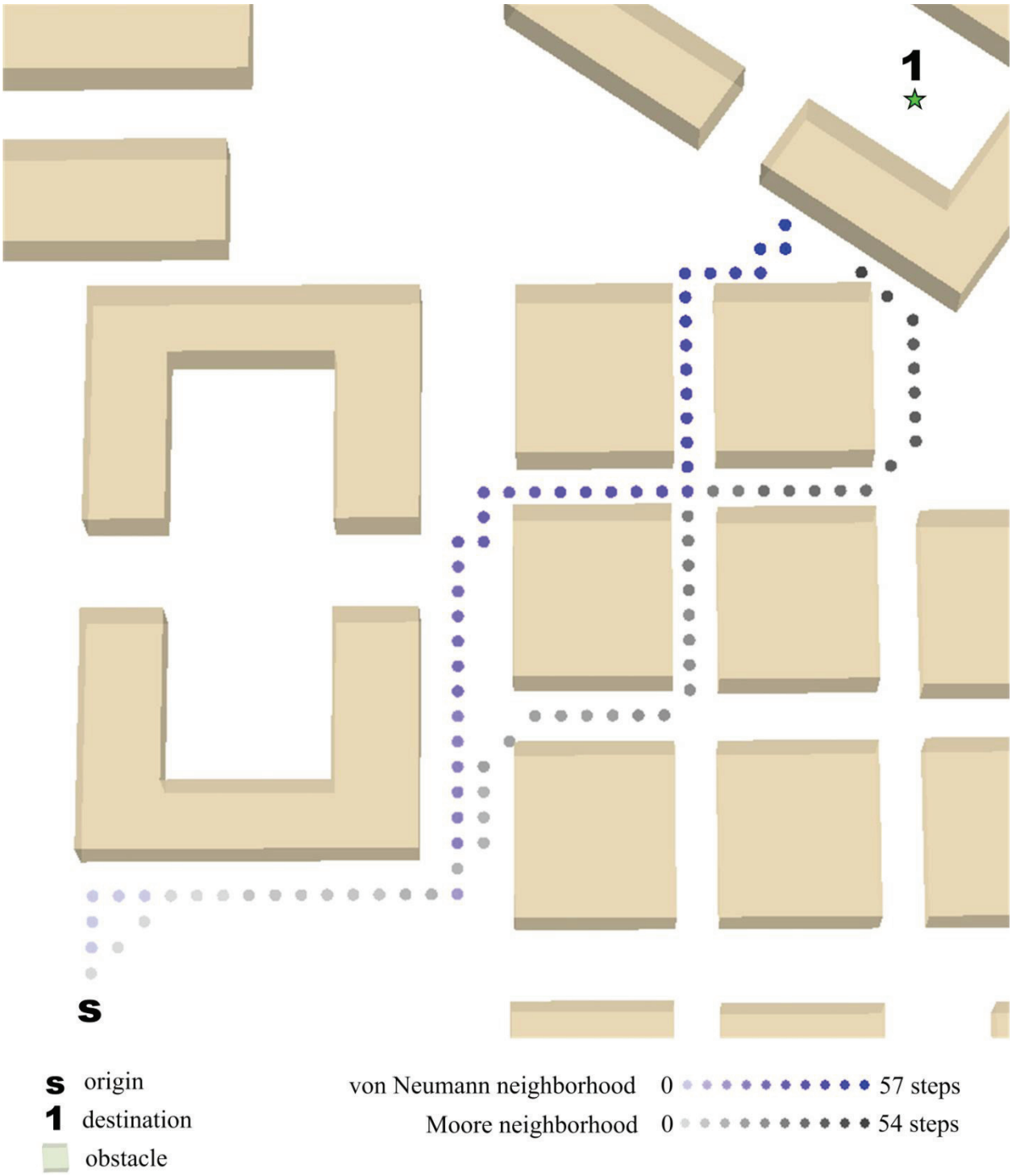

Figure 3. A hill-climbing algorithm is unable to resolve a simulated path to the first destination because it becomes trapped in a local minimum after 54 (or 57) steps: next-moves that are available to the algorithm are equidistant from the goal and the algorithm cannot choose between them. (The area represented above is covered by 2,500 units/pixels/rasters.)

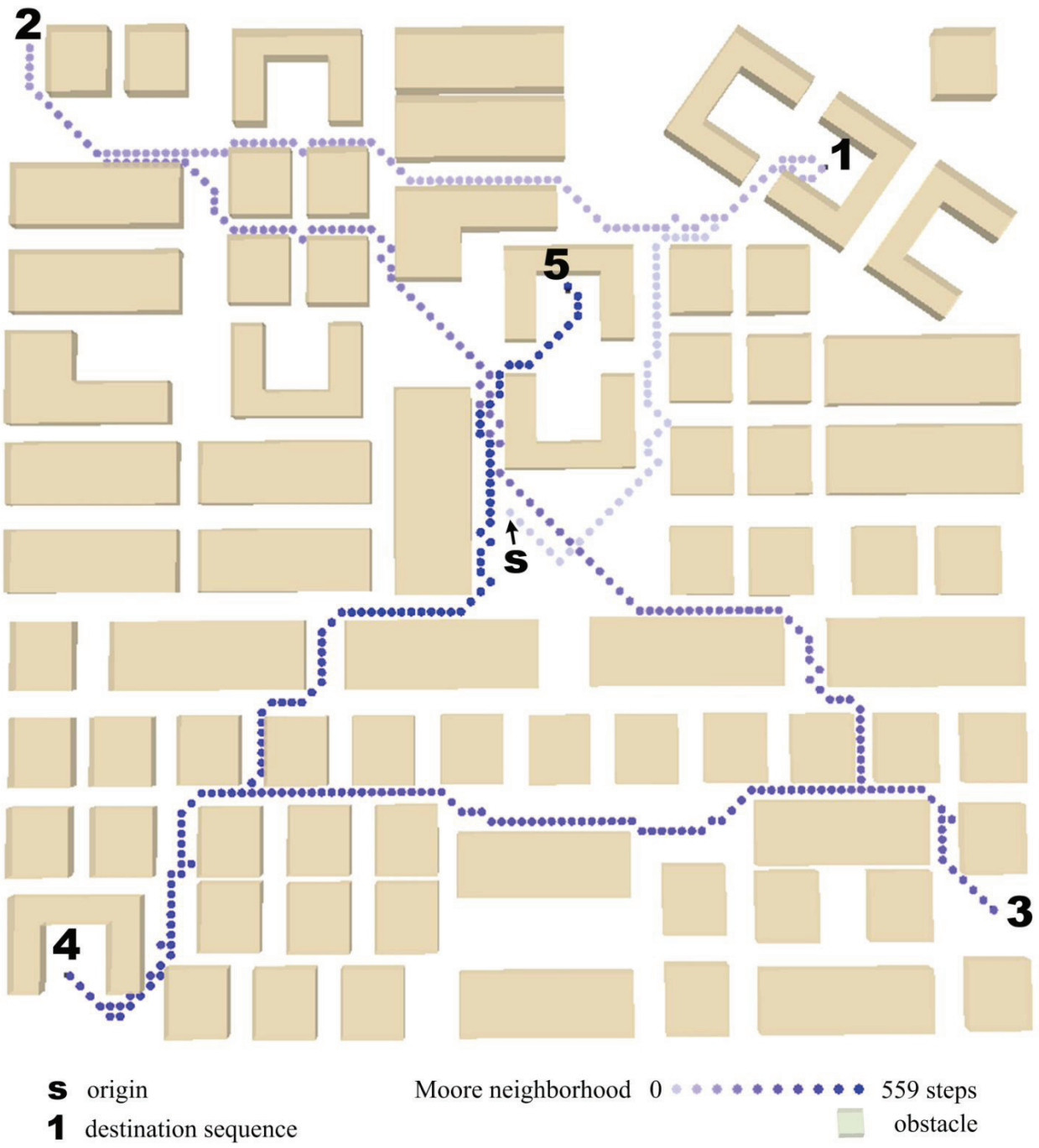

Figure 4 illustrates a simulated shortest path between an origin and five destinations, taken through a set of obstacles as determined by the Dijkstra algorithm with a Moore neighborhood filter, resolved in 14,460 moves. (The area represented above is covered by 10,201 units/pixels/rasters.)

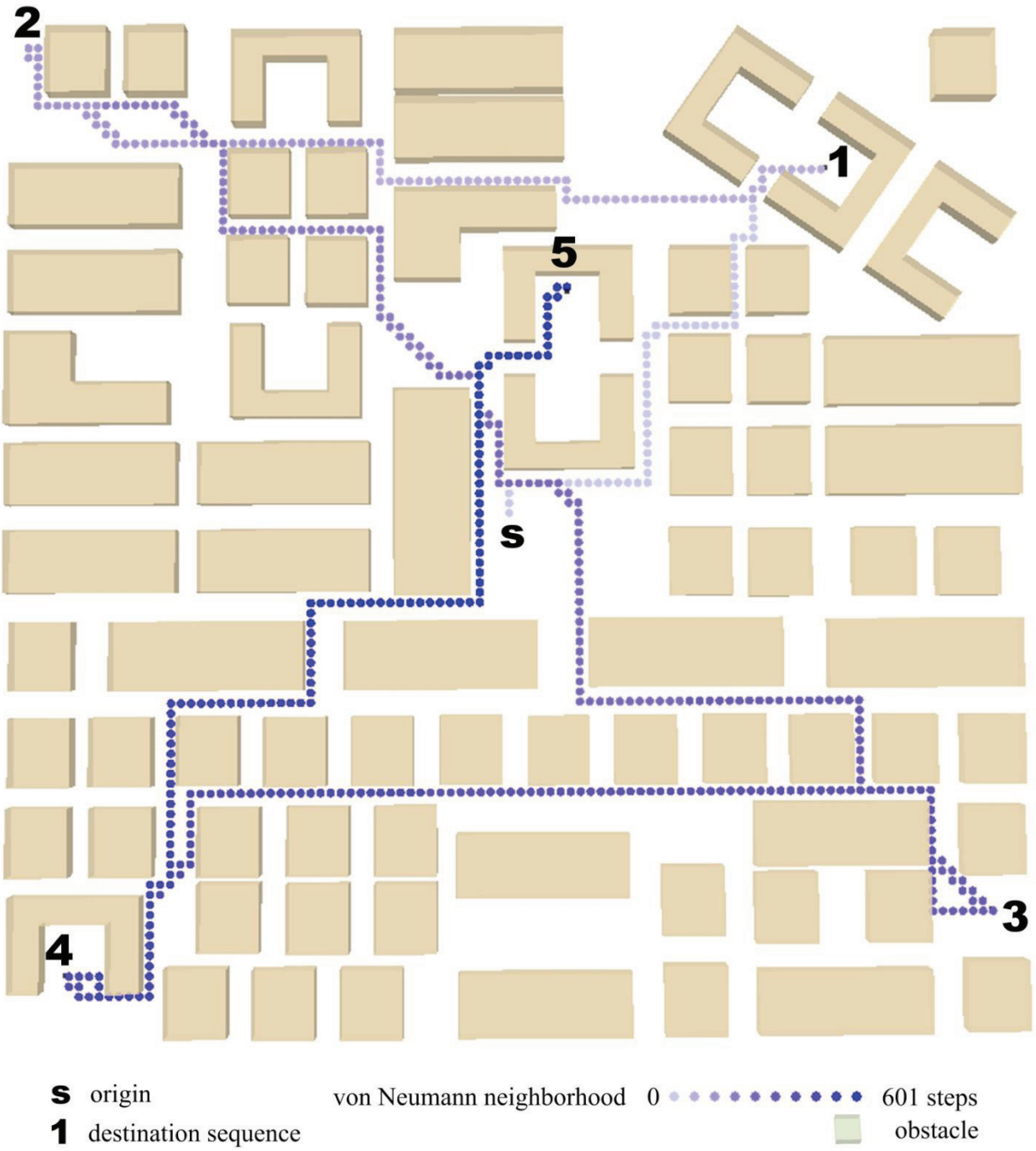

Figure 5 illustrates a simulated shortest path between an origin and five destinations, taken through a set of obstacles as determined by the A* algorithm with a von Neumann neighborhood filter, resolved in 18,037 moves. (The area represented above is covered by 10,201 units/pixels/rasters.)

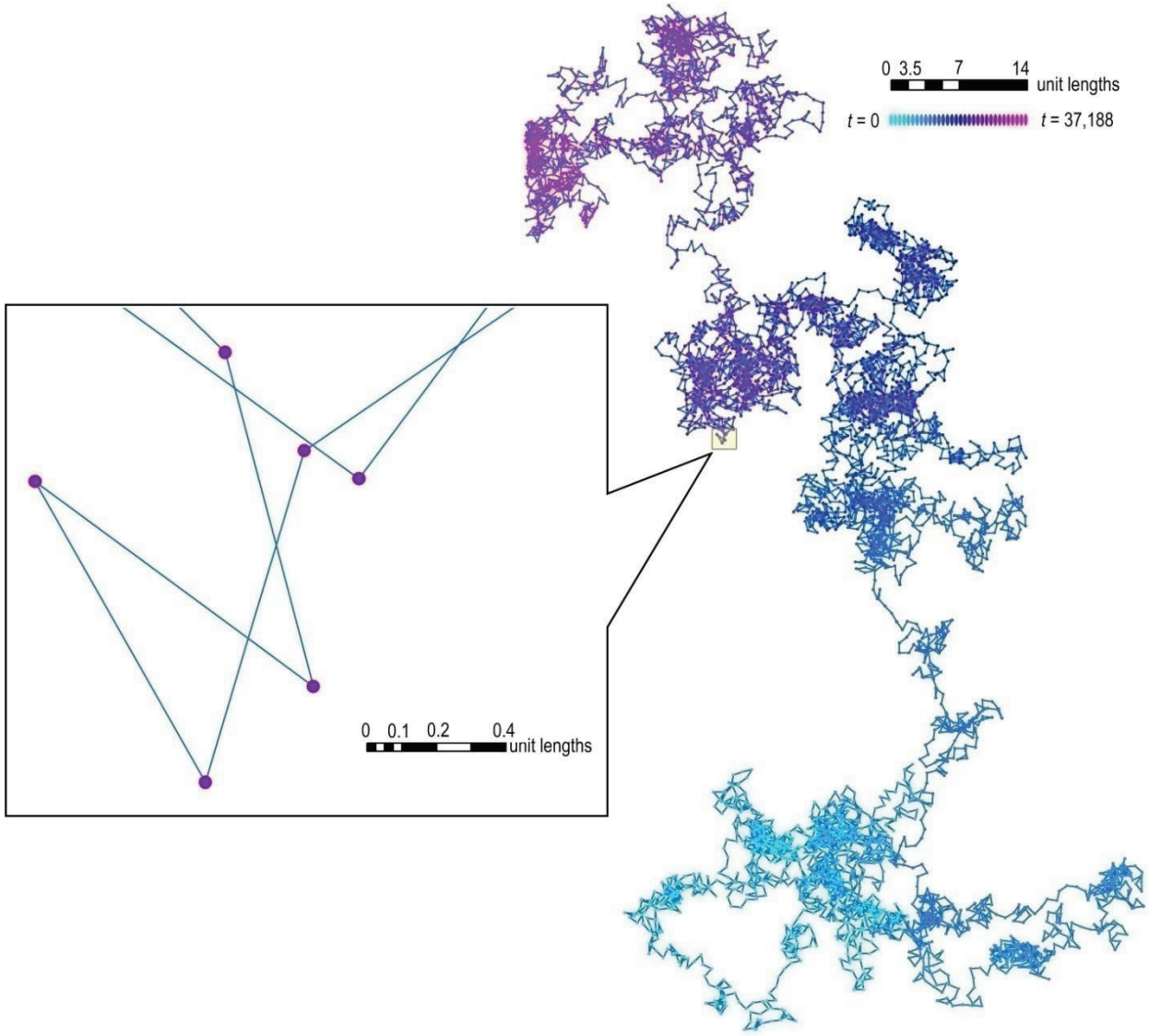

Figure 6. Simulated movement by (simple) random walk (in a flat, featureless plane).

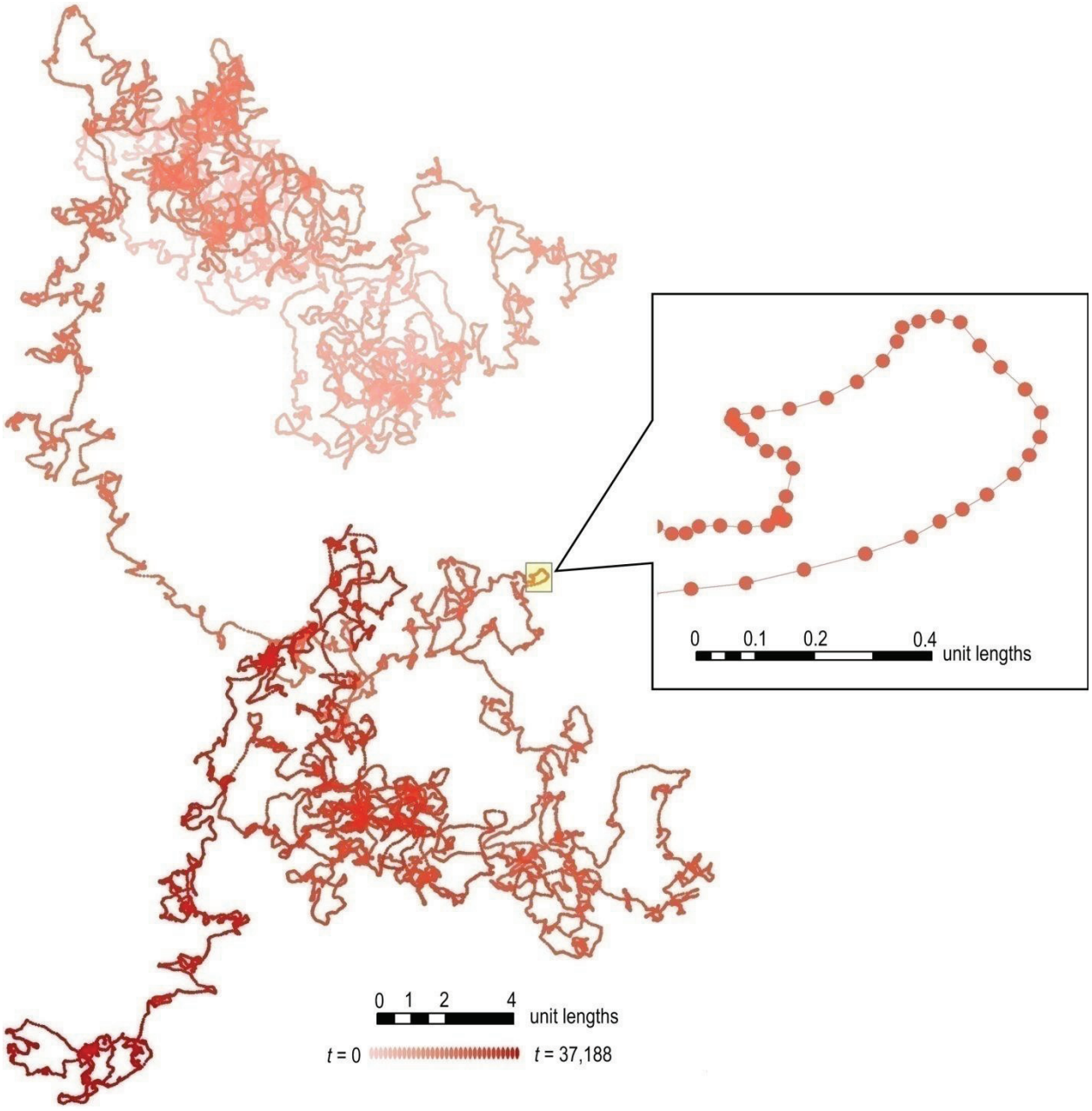

Figure 7. Simulated movement by Brownian motion (in a flat, featureless plane).

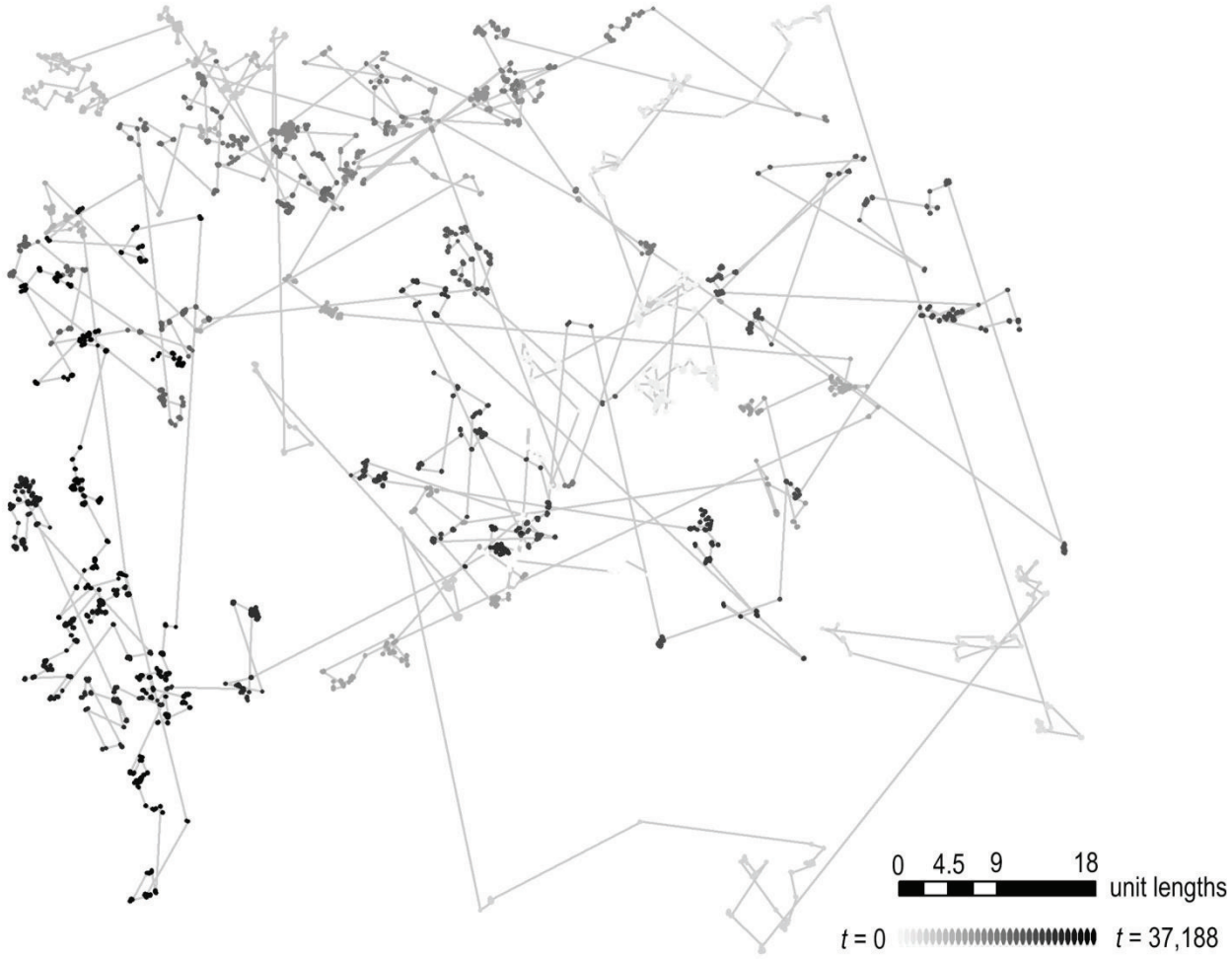

Figure 8. Simulated movement by Lévy flight (in a flat, featureless plane).

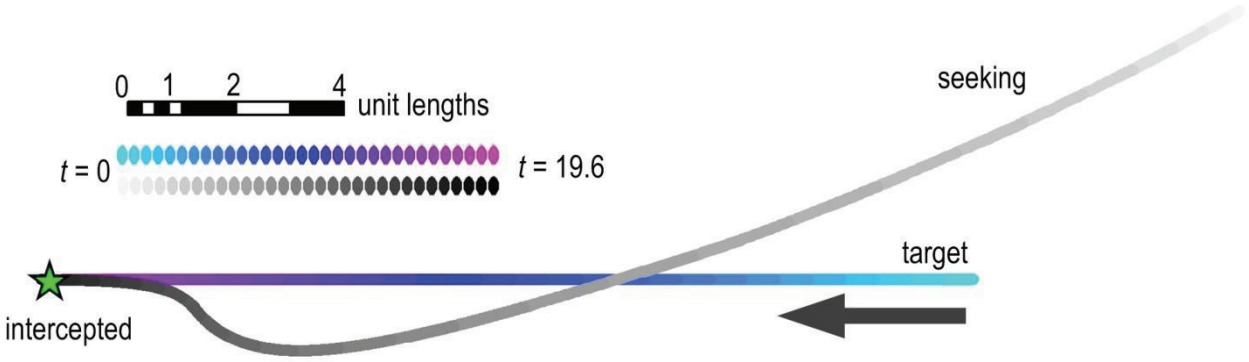

Figure 9. Simulated movement by dynamic seeking (in a flat, featureless plane).

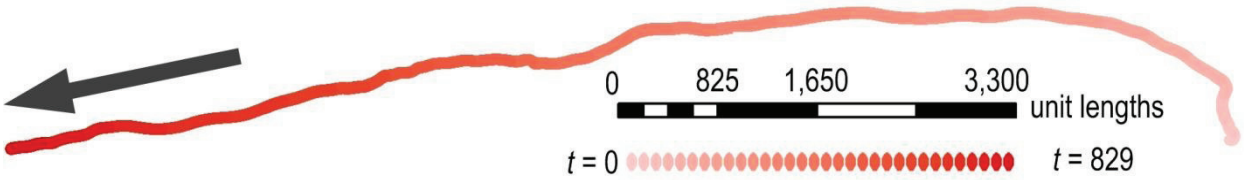

Figure 10. Simulated movement by dynamic wandering (in a flat, featureless plane).

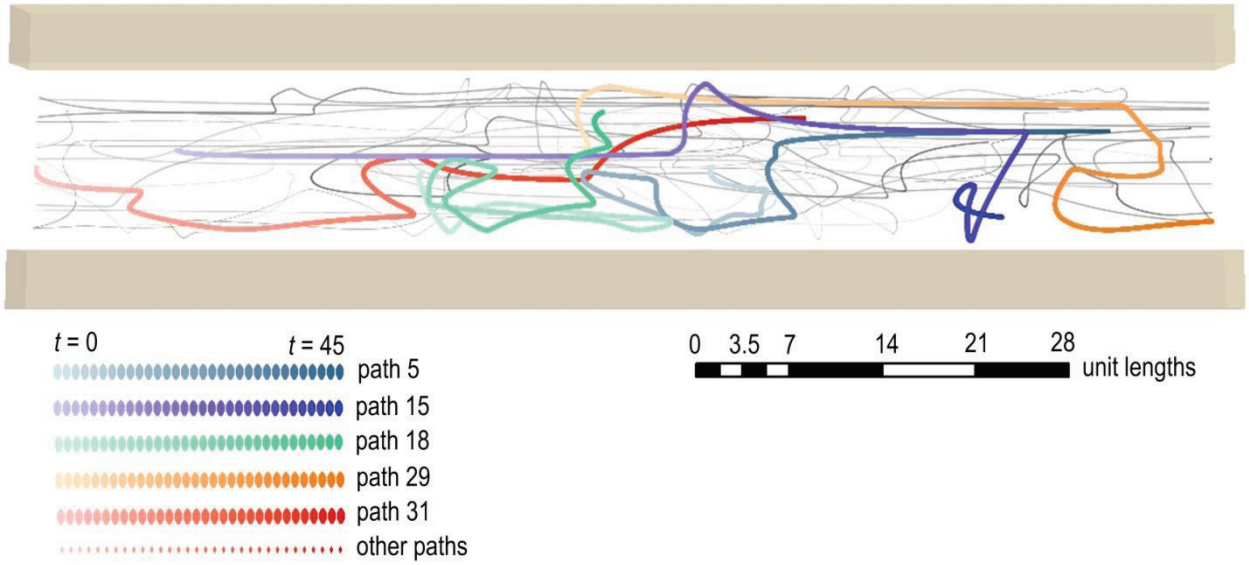

Figure 11. Simulated movement by social force.

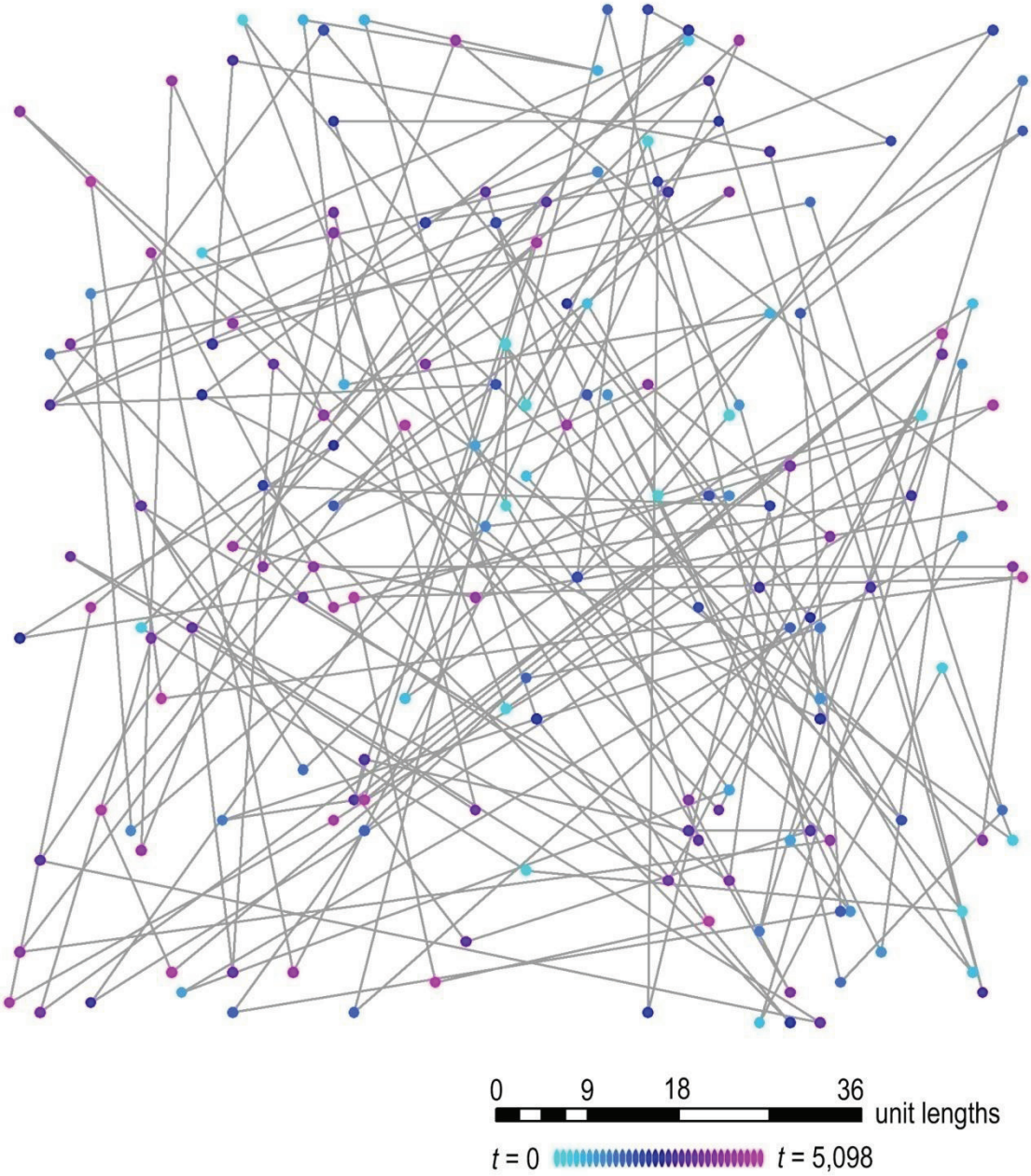

Figure 12. Simulated movement by hopping.

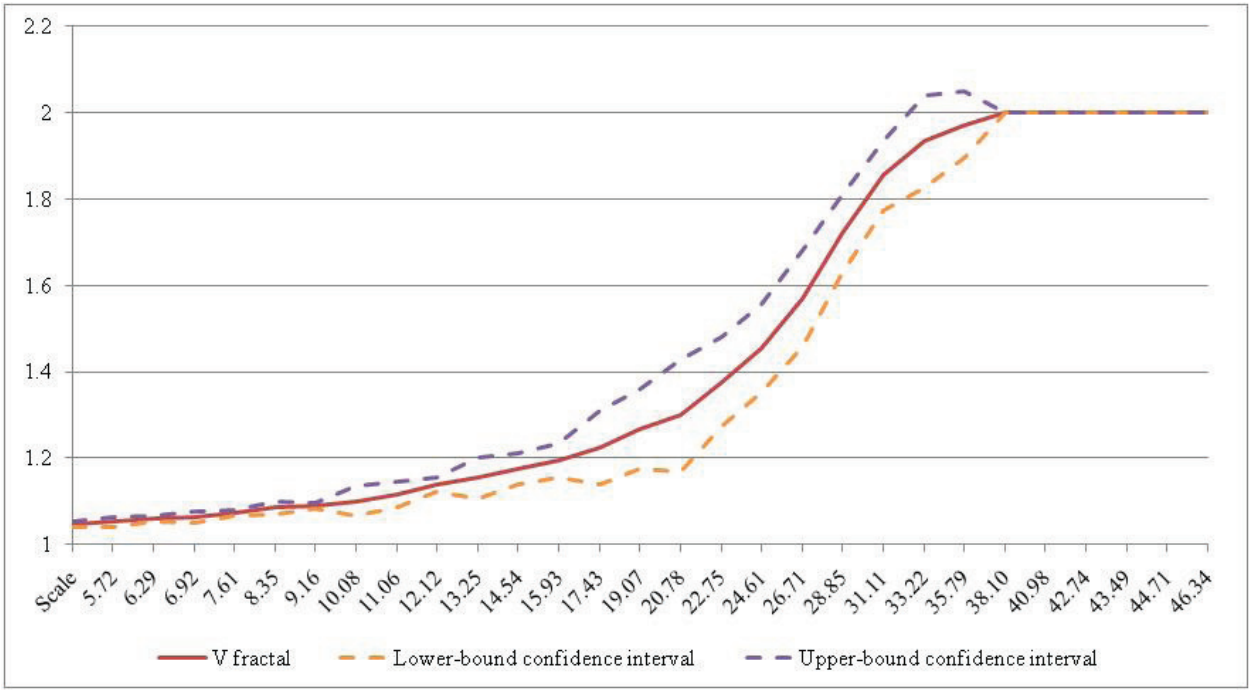

Figure 13. The VFractal profile for simulated movement by hopping.

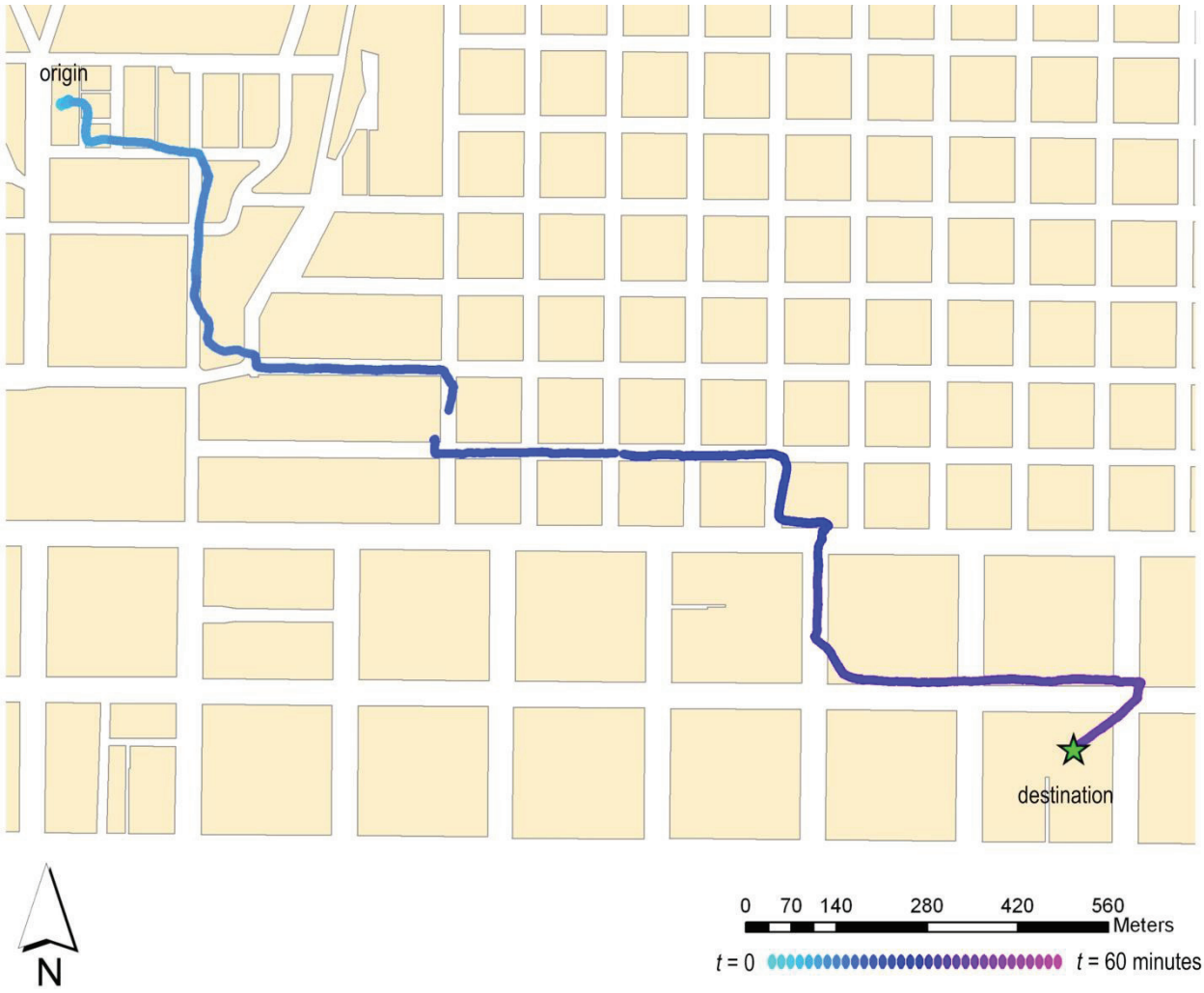

Figure 14. The path of walking data recorded for the downtown Salt Lake City, UT example.

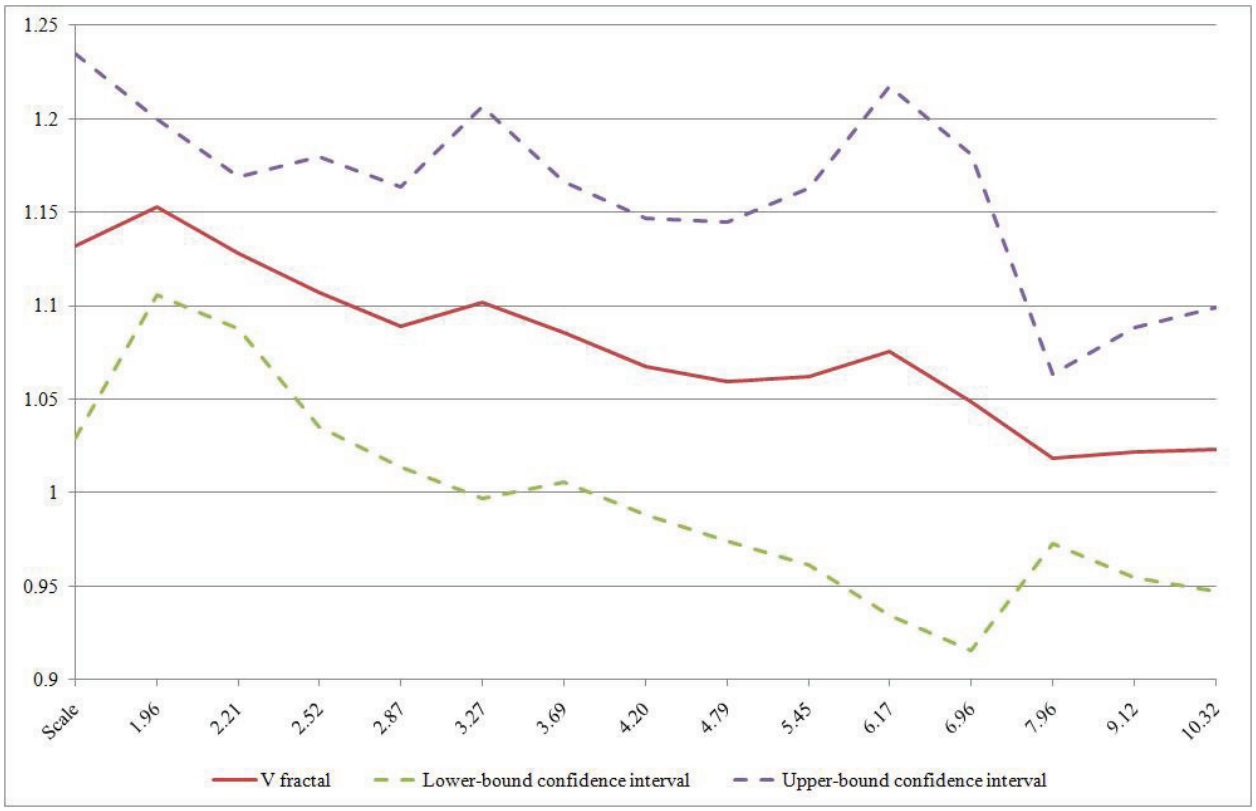

Figure 15. The VFractal profile of a real-world path for Shibuya crossing (path 1 in Appendix 1).

Tables

Table 1. Dijkstra's graph-search algorithm, as implemented in our model.

		$\boldsymbol{DIJKSTRA}(G, w, s)$
Initialize a search over directed or undirected graph, with vertices V and edges E, $G = (V, E)$, positive edge lengths $(l_e : e \in E)$, and edge weights w. Begin the search at origin $s \in V$. Record the distance d from the origin s. For each node u that is expanded, record its predecessor π (from an adjacency list $Adj[]$). Maintain a priority list Q as a queue of nodes that remain to be searched at any stage in the algorithm. Also maintain a list S_{list} of the nodes that form the shortest path from origin s to the destination. Initially, mark all nodes as unvisited ($WHITE$)	1	for each vertex $u \in V[G]$
	2	do $color[u] \leftarrow WHITE$
	3	$d[u] \leftarrow \infty$
	4	$\pi[u] \leftarrow NIL$
	5	$Q \leftarrow \emptyset$
	6	$S_{list} \leftarrow \emptyset$
Begin the search at the point of origin s and mark the node as visited ($GRAY$)	7	$color[s] \leftarrow GRAY$
Record its distance from the origin $s = 0$	8	$d[s] \leftarrow 0$
Record its predecessor node as NIL	9	$\pi[s] \leftarrow NIL$
Add s to the priority queue by popping stack Q	10	$ENQUEUE(Q, s)$
As long as more vertices remain to be explored…	11	while $Q \neq \emptyset$
Remove the previously-visited node from the priority queue by pushing stack Q	12	do $u \leftarrow DEQUEUE(Q)$
Find its adjacent nodes v connected by edge (u, v)	13	for each $v \in Adj[u]$
If that adjacent node v has not been evaluated	14	do if $color[v] = WHITE$
Mark the node v as explored, increment its total distance from the root node by 1, record node u as its predecessor, and add it to the priority queue Q	15	then $color[v] \leftarrow GRAY$
	16	$d[v] \leftarrow d[u] + 1$
	17	$\pi[v] \leftarrow u$
	18	$ENQUEUE(Q, v)$
Mark node u as resolved ($BLACK$)	19	$color[u] \leftarrow BLACK$
Add node u to the shortest path list S_{list}	20	$S_{list} \leftarrow S_{list} \cup \{u\}$

Table 2. Data collected for real-world walking paths.

Activity	**Walker age**	**Paths**	**Range**	**Time**	**Location**	**Environment**
Playing	2–5 years	13	30 m–145 m	Morning, afternoon	Tempe, AZ	Daycare center and playground
Lunch trip	25 years	1	682 m	Afternoon	Salt Lake City, UT	University campus
Work trip	30 years	1	2.8 km	Morning	Salt Lake City, UT	Medium-density, downtown residential
Shopping	30 years	1	4.6 km	Afternoon	Salt Lake City, UT	Open-air shopping mall
Browsing, art festival	25 years	1	2.9 km	Afternoon	Tempe, AZ	Medium-density, downtown retail
Crossing street	25 years	6	78 m–161 m	Evening	Shibuya crossing, Tokyo, Japan	High-density downtown
Recreational walking	25 years	2	1.2 km–6 km	Evening	Yokohama, Japan	High-density downtown
Browsing, light festival	22–30 years	21	67 m–2.2 km	Night	Phoenix, AZ	Zoo